

AD730613

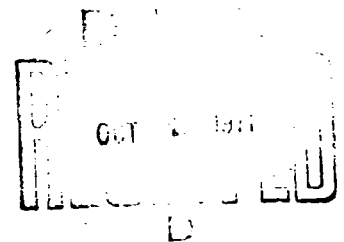
Report No. M & H 1.03

MATERIAL INSTABILITIES  
IN THE EXPERIMENTAL STUDY OF THE  
PLASTIC COMPRESSIBILITY OF SOME IMPORTANT METALS

K. C. Valanis and Han-Chin Wu  
Department of Mechanics and Hydraulics  
University of Iowa, Iowa City

Research sponsored by the Air Force Office  
of Scientific Research, Office of Aerospace  
Research, United States Air Force, under  
AFOSR ~~Contract~~ 70-1916.

August, 1971



Approved for public release;  
distribution unlimited.

Security Classification		
DOCUMENT CONTROL DATA - R & D <small>(Security classification of title, body of abstract and indexing annotation must be entered when the overall report is classified)</small>		
ORIGINATING ACTIVITY (Corporate author) University of Iowa Department of Mechanics and Hydraulics Iowa City, Iowa 52240		2a. REPORT SECURITY CLASSIFICATION UNCLASSIFIED
		2b. GROUP
1. REPORT TITLE MATERIAL INSTABILITIES IN THE EXPERIMENTAL STUDY OF THE PLASTIC COMPRESSIBILITY OF SOME IMPORTANT METALS		
4. DESCRIPTIVE NOTES (Type of report and inclusive dates) Scientific Interim		
5. AUTHOR(S) (First name, middle initial, last name) K. C. Valanis and Han-Chin Wu		
6. REPORT DATE August 1971	7a. TOTAL NO OF PAGES 50	7b. NO OF REFS 5
8a. CONTRACT OR GRANT NO AFOSR-70-1916		9a. ORIGINATOR'S REPORT NUMBER(S)
PROJECT NO. 9749 61102F 681304		9b. OTHER REPORT NO(S) (Any other numbers that may be assigned this report)
10. DISTRIBUTION STATEMENT Approved for public release; distribution unlimited.		
11. SUPPLEMENTARY NOTES TECH, OTHER		12. SPONSORING MILITARY ACTIVITY Air Force Office of Scientific Research(NM) 1400 Wilson Boulevard Arlington, Virginia 22209
13. ABSTRACT <p>The hypothesis of plastic incompressibility, which is pivotal in the development of the classical theory of plasticity has been tested by means of a series of simple tension tests on aluminum, copper and low carbon steel. The experimental measurements show conclusively that these metals are plastically compressible, the compressibility increasing with straining in the plastic region.</p> <p>A new phenomenon, termed lateral instability, has also been observed, consisting in an abrupt plastic flow in the transverse direction either immediately preceding or immediately following yield in the longitudinal direction, during a simple tension test on low carbon steel. To a less pronounced extent such a phenomenon has also been observed in the case of commercially pure aluminum.</p>		

### Abstract

The hypothesis of plastic incompressibility, which is pivotal in the development of the classical theory of plasticity has been tested by means of a series of simple tension tests on aluminum, copper and low carbon steel. The experimental measurements show conclusively that these metals are plastically compressible, the compressibility increasing with straining in the plastic region.

A new phenomenon, termed lateral instability, has also been observed, consisting in an abrupt plastic flow in the transverse direction either immediately preceding or immediately following yield in the longitudinal direction, during a simple tension test on low carbon steel. To a less pronounced extent such a phenomenon has also been observed in the case of commercially pure aluminum.

## I. Introduction

One of the assumptions of the classical theory of plasticity is that the material remains plastically incompressible while it undergoes plastic deformation. This implies that the hydrostatic response of the material remains elastic, (linearly, for small strains) even after yielding has occurred. This assumption also leads to the conclusion that Poisson's ratio\* tends to  $\frac{1}{2}$  as the plastic strain increases<sup>[1,2]</sup>.

In the present investigation the above assumption is evaluated critically by means of a series of simple tension tests on aluminum, copper and low carbon steel. We shall show in the following, that our experimental data do not support the hypothesis of plastic incompressibility. Moreover, Poisson's ratio does not tend to  $\frac{1}{2}$  as the plastic strain increases but, on the contrary, its value decreases and becomes smaller than its "elastic" value.

A newly observed form of material instability. The above statements on the observed behavior of Poisson's ratio, are true for copper and broadly true for aluminum and mild steel. However, in the case of mild steel (and to a lesser extent, aluminum) an unusual phenomenon, which we shall call LATERAL INSTABILITY, was observed for what is believed to be the first time. At least, to our knowledge no such phenomenon has ever been reported in the literature in the past.

---

\*It must be pointed out that, in this report, we do not regard Poisson's ratio as some fundamental physical property or function, but simply as the ratio of the algebraic values of the transverse and longitudinal strains, in a uniaxial test. On the other hand because the experiments reported here were carried out in the small strain range, Poisson's ratio is a convenient quantity to work with, since it can be used to relate directly the uniaxial to the volumetric strain; the latter is an important parameter in our investigation.

Lateral instability is defined by one of the following two observed sequences of events during a simple tension test.

- (a) As the yield point of a low carbon steel specimen is reached, the material begins to flow longitudinally (i.e., in the direction of applied stress) and one observes the usual increase in longitudinal strain while the longitudinal stress remains constant. However an abrupt occurrence of plastic flow in the transverse direction has also been observed, just after longitudinal flow has ceased and strain-hardening has begun.
- (b) Abrupt transverse flow occurred just before the onset of longitudinal flow.

It is significant that no transverse flow has been observed during the process of longitudinal flow. A more detailed discussion of this phenomenon will be given in text.

In the case of aluminum the onset of lateral plastic flow was not abrupt, but what was observed amounted to a significant increase in the transverse strain during a relatively small increment in longitudinal strain. A quantitative plot of these events is shown in later figures.

Loading-unloading loops have also been observed in some of the tests. It will be shown in later sections that loops are also obtained in plots of transverse strain versus longitudinal strain, and hydrostatic stress versus volumetric strain.

## II. Materials and Specimens

Altogether three metallurgically important metals were tested. They were commercially pure aluminum, electrolytic tough pitch copper and low-carbon steel. The aluminum specimens were sheared from an 1100-0 aluminum sheet, all the copper specimens were cut out of an electrolytic tough pitch copper 110 (99.9<sup>+</sup>% copper) bus bar, and the steel specimens were cut from a cold drawn C 1018 flat. The nominal dimension of all the aluminum and copper specimens was  $\frac{1}{8}$ " x  $\frac{3}{4}$ " x 15" and that of all the low-carbon steel specimens was  $\frac{1}{8}$ " x  $\frac{1}{2}$ " x 12". All the specimens of the same metal were considered to be identical prior to the heat treatment. These specimens have been divided into several groups, according to the annealing temperatures and purposes of study. They are listed in Table I.

### III. The Equipment and Strain Measurements

All tests were conducted at room temperature on a Tinius Olsen Lo Cap universal testing machine with strain gage load cell weighing and equipped with a Tinius Olsen Model 51 electronic recorder. The load readings on the dial indicator were calibrated against a Tinius Olsen proving ring with the electrical vibrating reed.

A Tinius Olsen S-400-2AB extensometer was used to measure the longitudinal strains of all the specimens except those of group III of aluminum. This is an averaging type extensometer with a gage length of two inches. The accuracy of the extensometer is  $\pm 0.0001$  in/in as guaranteed by the manufacturer and was calibrated against the SR-4 electric strain gages of type A-7 which have the accuracy of  $2 \times 10^{-5}$  in/in. The load vs. longitudinal strain  $\epsilon_x$  curves were plotted by the Model 51 recorder during experiments.

To measure the transverse strains  $\epsilon_y$ , a SR-4 electric strain gage of type A-7 was transversely put on one side of each specimen. The transverse strain was then read directly from a SR-4 portable strain indicator at the accuracy of  $2 \times 10^{-5}$  in/in.

The strain measurements of the specimens of group III of aluminum were specially arranged for greater accuracy. A-7 type strain gages were longitudinally and transversely glued on both sides of each specimen belonging to this group, in order to cancel out the bending effect. The strain reading of each gage was then obtained from a SR-4 portable strain indicator with the help of a BLH Model 225 switching and balancing unit. Finally, the average value of the readings of the two longitudinally arranged strain gages gives us the longitudinal strain  $\epsilon_x$ , and the average value of the



readings of the two transversely arranged strain gages gives us the transverse strain  $\epsilon_y$ .

#### IV. Description of Tests and Results

##### Experiments on Aluminum

The first group of aluminum specimens was tested under the "as-received" condition. During the tests, the Tinius Olsen machine was operated at a constant rate of crosshead separation. The rate was  $8 \times 10^{-4}$  in/sec, which corresponds to a strain-rate of approximately  $5 \times 10^{-5}$  in/in/sec for the specimens used. The recorder traced out the load versus  $\epsilon_x$  curve as readings of load and of transverse strain were taken simultaneously at predetermined readings of load, at small longitudinal strains, and at predetermined readings of longitudinal strains, when the strain was large.

The stress-strain curves are shown in Fig. 1, in which the curve for specimen #1 is identical to that for specimen #2. Fig. 2 shows the relations between the transverse and the longitudinal strain, and Fig. 3 shows the hydrostatic stress ( $\times 3$ ) versus the volumetric strain curve for aluminum of group I. A loading-unloading loop was generated at the end of each test, and we obtain loops, which is similar to the hysteresis loops, in the curves of Figures 2 and 3 (not shown). More observations and discussions of the loops will be presented later in this report. The large increase of  $-\epsilon_y$  at a longitudinal strain of approximately 2.5% (see Fig. 2) corresponds to a case of "mild" lateral instability as compared to the "strong" lateral instability observed in low-carbon steel. We shall make more observations later about the lateral instability of aluminum.

The second group of aluminum specimens was tested exactly in the same way as those of group I, except that the specimens were first annealed at a temperature of 600°F for two hours and then oven cooled to the room temperature before testing. This annealing process removes most of the effects due

to cold work, and the material can thus be considered as isotropic. The stress-strain curves for specimens Al #3 and Al #4 are shown in Fig. 4, in which the two curves are indistinguishable. We notice, however, that the material is considerably softened due to the heat treatment.

To see the sudden increase in magnitude of the transverse strain at a longitudinal strain of approximately 2.2%, which has been an observed fact in the test of group I, this series of tests was carried out to the extent that the longitudinal strain at the time of termination of the test was approximately 9%. Here, again, we have observed a sudden increase in  $-\epsilon_y$  at a longitudinal strain of approximately 2.2%. This phenomenon has been observed both for specimens Al #3 and Al #4.

The  $-\epsilon_y$  vs.  $\epsilon_x$  curves are plotted in Fig. 5, and the  $\sigma_{kk}$  vs.  $\epsilon_{kk}$  curves are given in Fig. 6. The sudden increase of the transverse strain in Fig. 5 gives rise again to the sudden decrease of the volumetric strain in Fig. 6 which corresponds to the lateral instability mentioned earlier. In this series of test, the loopings of the curves are once more present in all the figures concerned (not shown). These loopings are due to the loading-unloading test conducted at the end of each study.

It is important to point out, that aside of the sudden change of Poisson's ratio immediately following yielding, Poisson's ratio remains approximately constant throughout the range tested. Poisson's ratio in the plastic range is defined in the present investigation by the expression

$$\nu = - \frac{\epsilon_y}{\epsilon_x}$$

which, in fact, is also used in elasticity (see footnote in the introduction).

Group III of the aluminum specimens was tested quasi-statically, i.e., readings were taken after the machine had been stopped and time of 5 minutes

had already elapsed. By doing this, it is believed that the results obtained are time independent. As it has already been described earlier in this report that four strain gages were applied to each specimen of this series to eliminate the bending effect due to the possible eccentricity of the loading arrangement. The comparison of the present results (shown in Figures 7-12) with those obtained earlier in groups I and II of the aluminum specimens shows that reliable data can be obtained without the complicated strain gage set-ups of group III. In fact, the grips of the Tinius-Olsen machine are of the self-aligning type, therefore, eccentricity is to be expected at its minimum.

Loops are again present in all the figures concerned (Figures 7-12). It is seen from Figures 9 and 10 that Poisson's ratio decreases again drastically immediately following yielding.

The fact that all the curves in Figures 3, 6, 11 and 12 bend over toward the  $\epsilon_{kk}$ -axis leads to the conclusion that aluminum is plastically compressible, at least when the hydrostatic stress is of a tensile nature. The assumption of plastic incompressibility in the classical theory of plasticity would lead to a linear relation between hydrostatic stress and volumetric strain; this apparently is not the case.

#### Experiments on Copper

The experiments on group I of the copper specimens were designed to further study the loops which we had observed in the tests of aluminum specimens. These specimens of copper were tested under the "as-received" condition. The rate of crosshead motion was kept constant ( $8 \times 10^{-4}$  in/sec) during this series of test. The loading-unloading curves for specimens Cu #1 and Cu #2 are shown in Figures 13 and 14, and the corresponding  $-\epsilon_y$  versus  $\epsilon_x$  curves are shown in Figures 15 and 16. We see here again that loops are definitely in existence and that, after a loop has been completed, the curve of  $-\epsilon_y$

versus  $\epsilon_x$  is virtually a continuation of the original  $-\epsilon_y$  versus  $\epsilon_x$  curve. The plots of  $\sigma_{kk}$  vs.  $\epsilon_{kk}$  for these specimens are given in Figures 17 and 18.

The copper specimens of group II were tested in exactly the same way as those of the aluminum specimens of group II, except that the annealing temperature was 750°F. The results are shown in Figures 19, 20 and 21. We remark that in contrast with the aluminum specimens we do not observe the sudden increase in the magnitude of the transverse strain for all the copper specimens concerned. As a result, Poisson's ratio is approximately a constant throughout the range tested.

Experiments were conducted on group III of the copper specimens under quasi-static conditions, i.e. readings were taken after the machine had been stopped and 5 minutes had elapsed. The results of this series are given in Figures 22, 23 and 24. We again observe no sudden increase in the magnitude of the transverse strain and that Poisson's ratio is virtually constant throughout the range tested.

The tests on copper specimens of groups I, II and III show conclusively that copper is also plastically compressible, as it is seen easily from Figures 17, 18, 21 and 24; otherwise these plots would have been straight lines.

#### Experiments on Low Carbon Steel

The same experimental procedure as described above was followed when the five low-carbon steel specimens were tested. All the five specimens were annealed, prior to tests, at a temperature of 1250°F for one hour and then oven cooled to room temperature. Thus, all the specimens can be considered to be identical and the material can be considered to be isotropic.

The tests were carried out under quasi-static conditions, and a typical stress-strain curve for these specimens is given in Fig. 25. In Fig. 26, the

relation between the transverse strain and the longitudinal strain is plotted for all the five specimens. It is seen that aside of the portion reflecting "lateral instability" the curve is almost a straight line. Of all the specimens tested in this series, three of them (#1, #2 and #4) showed lateral instability before the occurrence of the longitudinal plastic flow, and follow the path OABDE in Fig. 26. The rest of the specimens (#3 and #5) experienced lateral instability immediately after the longitudinal plastic flow had been accomplished, i.e., lateral instability had occurred before the material strain-hardened. In this case, curve OACDE of Fig. 26 is followed.

We conjecture that had the material been homogeneous as well as isotropic then longitudinal and transverse flow would have taken place simultaneously. Since in practice this is rarely true, the order in which these flows occur must then be decided by slight differences in the directional properties of the specimen.

To ensure the correctness of our observation about the lateral instability as a material property of low-carbon steel. The transverse dimension of all specimens was measured after the experiments by means of a micrometer. The permanent transverse strains were then calculated referring to the original dimensions of the specimens. The results checked favorably (with less accuracy, of course) with those obtained by means of electric strain gages. Two of the five experiments (#2 and #4) were terminated right after the occurrence of the transverse plastic flow and before much longitudinal flow had occurred, in order for us to study the lateral instability more closely. Measurements by means of both electric strain gages and micrometer showed that large amount of plastic flow did occur transversely at yielding. If it was not for the transverse plastic flow, the transverse permanent strains would have been very small for these two specimens.

The relation between the hydrostatic stress and the volumetric strain is shown in Figures 27-31. The alphabetical order of letters in the figures denotes successive states of the material during the tests. The last letter in the figure gives us the position where the corresponding test was terminated. It is seen that the lateral instability corresponds to a sudden decrease of volumetric strain. In the case when lateral instability occurs before the longitudinal plastic flow, the volumetric strain could become negative! A very strange result!

However, a similar phenomenon was observed by Bridgman<sup>[6]</sup>. He investigated, by means of a dilatometer, volume changes during simple compression in the plastic range, in various materials, such as mild steel, Norway iron, cast iron and rock (soapstone, marble and diabase). He observed an increase in volume under conditions of compressive hydrostatic stress, when the axial compressive stress exceeded its yield value.

#### V. On the Accuracy of the Experimental Measurements

It is to be noted that it is impossible to glue a strain gage on the specimen such that the strain gage makes an angle of exactly  $90^\circ$  degrees with the longitudinal direction of the specimen. Slight errors are always possible, and these errors tend to make the readings of transverse strain smaller than it should be. These are, however, small since the gages are in the principal strain directions. According to Perry and Lissner<sup>[3]</sup>, a 2 degree error in gage alignment would only result in an error of less than 1%.

Our purpose in the present experimental study is not the determination of the exact value of Poisson's ratio. Our primary concern is the trend in the variation of Poisson's ratio as the longitudinal strain increases. For this reason, the above mentioned deviations due to the misalignment of the transverse strain gages are not important, since they hardly affect the broad trends in the variation of Poisson's ratio, which are of interest here.

Slight scattering of some of our experimental data for different specimens may be attributed partially to the above mentioned misalignments of the transverse strain gages. We notice, however, that our data are very consistent in general, and the slight scattering of data occurs only in the case of copper specimens #5 and #6. Even in these cases where data are scattered slightly, the curve for each specimen is itself smooth, which indicates that scattering is due to a large extent to variability in the properties of the specimens.

Of course corrections must also be made on the readings of the transverse strain  $\epsilon_y$  due to the effect of transverse sensitivity of the electric strain gages. The transverse sensitivity factor for A-7 strain gage is given by



Perry and Lissner<sup>[3]</sup> as  $k = -0.01$ . The error, which is defined by  $e = \frac{\epsilon_c - \epsilon}{\epsilon}$ , where  $\epsilon_c$  is the apparent strain and  $\epsilon$  is the true strain, is 3% for a Poisson's ratio of 0.3 and is 2.6% for a Poisson's ratio of 0.33. It is equivalent to saying that  $\epsilon = 0.971 \epsilon_c$  for material with Poisson's ratio of 0.3 and  $\epsilon = 0.984 \epsilon_c$  for material with Poisson's ratio of 0.33. We have thus seen that the true transverse strain is 2.9% smaller than the apparent transverse strain when  $\nu = 0.30$ , and is 1.6% smaller than the apparent transverse strain when  $\nu = 0.33$ . This correction is however in a different direction from the one due to the misalignment of the strain gages, therefore some of the errors should cancel out.

Stang, Greenspan and Newman<sup>[4]</sup> reported in as early as 1946 their experimental study on Poisson's ratio of aluminum alloys 24 ST and 24 SRT, chrome-molybdenum steel plate and structural and fully killed low-carbon steel plate. In all cases these authors reported the increase of Poisson's ratio beyond its initial (elastic) value throughout the longitudinal strain range tested. This observation is not in agreement with the present findings.

We like to mention that the above discussed misalignment in the transverse strain gages also existed in the tests by Stang et al<sup>[4]</sup>. In addition to this, as it was pointed out by these authors themselves in their report, there were large discrepancies in the values of Poisson's ratio obtained by them for two nominally identical specimens.

Finally, from a thermodynamic point of view the hydrostatic stress versus volumetric strain curve should bend over toward the  $\epsilon_{kk}$ -axis<sup>[5]</sup>; this agrees with our own observations.

## VI. Conclusions

The following conclusions can be drawn from the present experimental study:

- (1) The curve of hydrostatic stress versus volumetric strain bends over toward the volumetric strain axis for all three materials tested. This implies that the commercially pure aluminum, the electrolytic tough pitch copper and the low-carbon steel are plastically compressible, (at least when the hydrostatic stress is of a tensile character) and that the most important assumption in the classical theory of plasticity concerning the plastic incompressibility of material lacks experimental justification.
- (2) Lateral instability occurs weakly in the case of aluminum and occurs strongly in the case of low-carbon steel. Lateral instability always follows the longitudinal plastic flow for aluminum, whereas two possibilities arise in the case of low-carbon steel—lateral instability may precede or follow the longitudinal plastic flow as dictated by the anisotropy of the material. No phenomenon of lateral instability has been observed for the copper specimens tested.
- (3) The lateral instability corresponds to a decrease in volume due to a slight increase in load for the case of aluminum, and corresponds to a sudden decrease in volume while the load remains constant for the case of low-carbon steel. Where the lateral instability occurs, Poisson's ratio has a large increase.
- (4) Poisson's ratio for the commercially pure aluminum decreases considerably after yield has occurred, from an initial value of 0.30 to a

value as low as 0.06 corresponding to a longitudinal strain of approximately 2%; beyond this point it increases continuously and at an axial strain of 3% it reaches a value of 0.15 which remains approximately constant up to  $\epsilon_x = 9\%$ .

- (5) For the electrolytic copper, Poisson's ratio decreases continuously with  $\epsilon_x$  from a value of 0.35 to a value of 0.3 at  $\epsilon_x = 9\%$ .
- (6) For the low-carbon steel, two possibilities prevail. If the lateral instability occurs before the longitudinal plastic flow then Poisson's ratio increases suddenly at yielding from its initial value of 0.29 to a value as high as 6.0. It then decreases gradually and reaches a value of 0.3 at  $\epsilon_x = 3\%$ . Beyond this point, Poisson's ratio remains approximately constant up to  $\epsilon_x = 9\%$ . If the lateral instability occurs after the longitudinal plastic flow, then Poisson's ratio decreases considerably after yield has occurred from an initial value of 0.29 to a value as low as 0.02 corresponding to a longitudinal strain of approximately 2.5%, beyond this point, it increases continuously and at an axial strain of 3% it reaches a value of 0.3 which remains approximately constant thereafter.
- (7) Loops similar to the hysteresis loops are present in curves obtained by plotting  $-\epsilon_y$  against  $\epsilon_x$  and also in curves of  $\sigma_{kk}$  against  $\epsilon_{kk}$  for all three materials tested.

Acknowledgement

The authors wish to express their appreciation to Mr. Hyo Kim of his very capable assistance with the experimental work and the preparation of the graphs.

References:

- [1] Hill, R., "The mathematical theory of plasticity", Oxford, 1950.
- [2] Naghdi, P. M., "Stress-strain relations in plasticity and thermo-plasticity", PLASTICITY, edited by E. H. Lee and P. S. Symonds, Pergamon Press, London, 1960.
- [3] Perry, C. C. and Lissner, H. R., "The strain gage primer", McGraw-Hill, New York, 1962.
- [4] Stang, A. H., Greenspan, M. and Newman, S. B., "Poisson's ratio of some structural alloys for large strains", Journal of Research, National Bureau of Standards, 37, 211-221, 1946.
- [5] Valanis, K. C., "A theory of viscoplasticity without a yield surface", Archives of Mechanics - Archiwum Mechaniki Stosowanej, 23, 4 (1971) (in press).
- [6] Bridgman, P. W., "Volume changes in simple compression", J. App. Phys. 20, 1241, (1949).

TABLE I

Metal	Group	Specimen	Heat Treatment	Remarks
Al 1100-0	I	#1	No	Constant strain-rate test
		#2		
	II	#3	Annealed at 600°F for 2 hrs. and then oven cooled to room temperature	Constant strain-rate test
		#4		
	III	#5	Annealed at 600°F for 2 hrs. and then oven cooled to room temperature	Quasi-static test, loading- unloading loops observed strain gages on both sides of specimens.
		#6		
Cu 110	I	#1	No	Constant strain-rate test, loading-unloading loops observed.
		#2		
	II	#3	Annealed at 750°F for 2 hrs. and then oven cooled to room temperature	Constant strain-rate test
		#4		
	III	#5	Annealed at 750°F for 2 hrs. and then oven cooled to room temperature	Quasi-static test
		#6		
Low- Carbon Steel C1018		#1		
		#2		
		#3	Annealed at 1250°F for 1 hr. and then oven cooled to room temperature	Quasi-static test, lateral instability observed
		#4		
		#5		

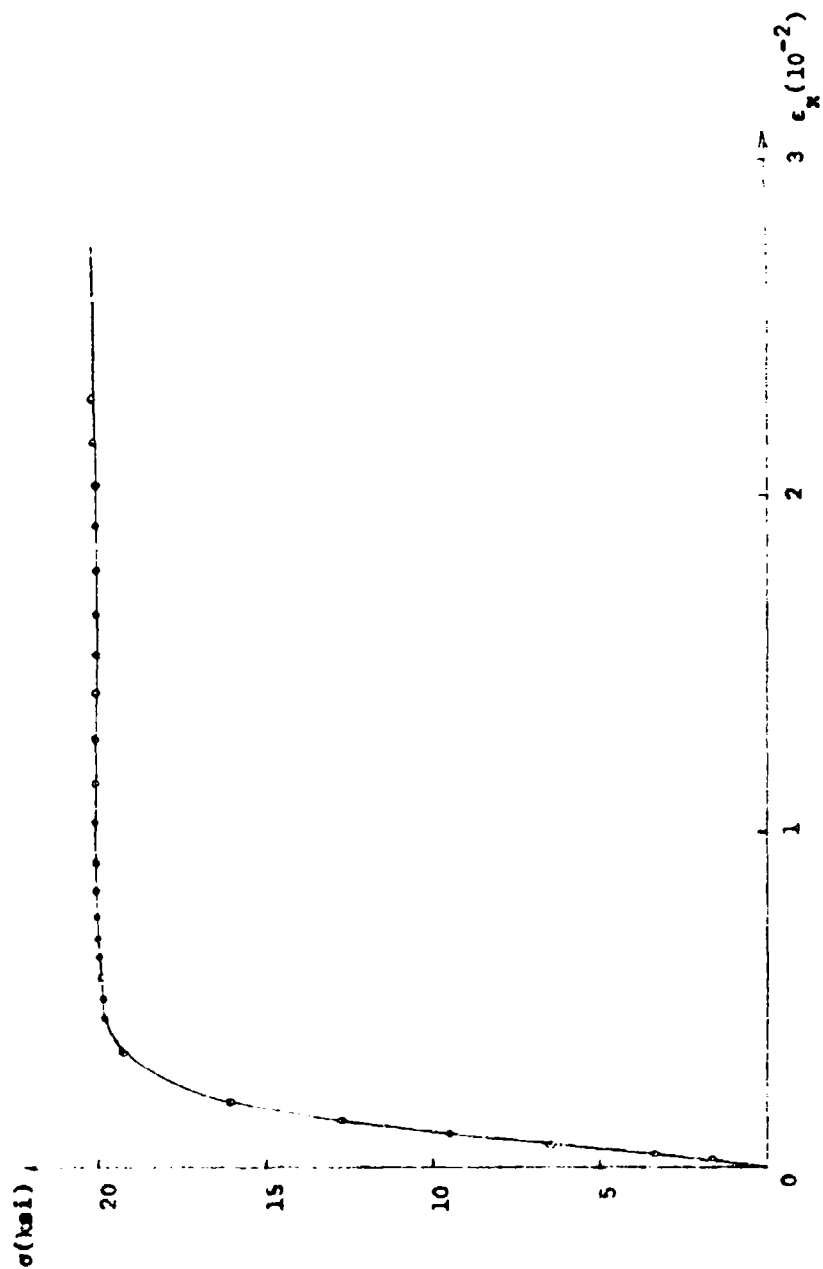


Figure 1 The stress-strain curve for aluminum of group I

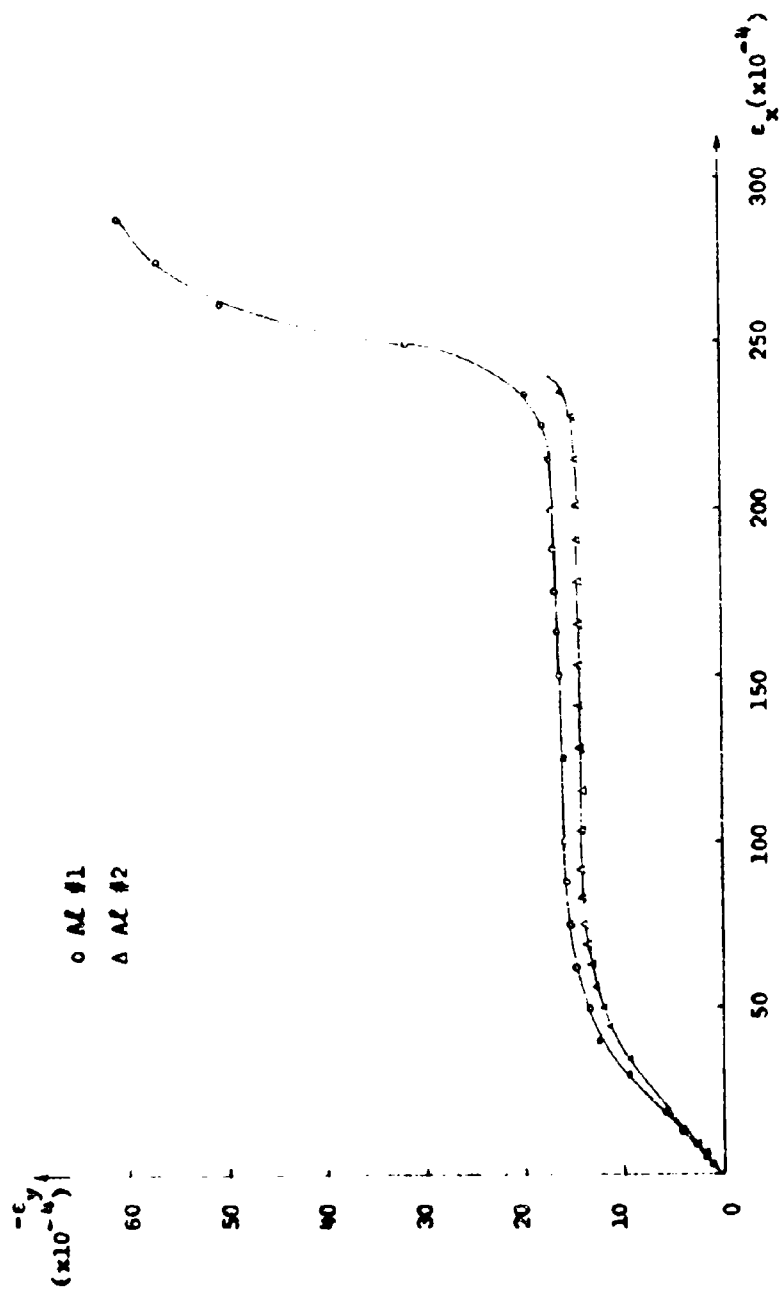


Figure 2 Relations between transverse and longitudinal strain for aluminum of group 1



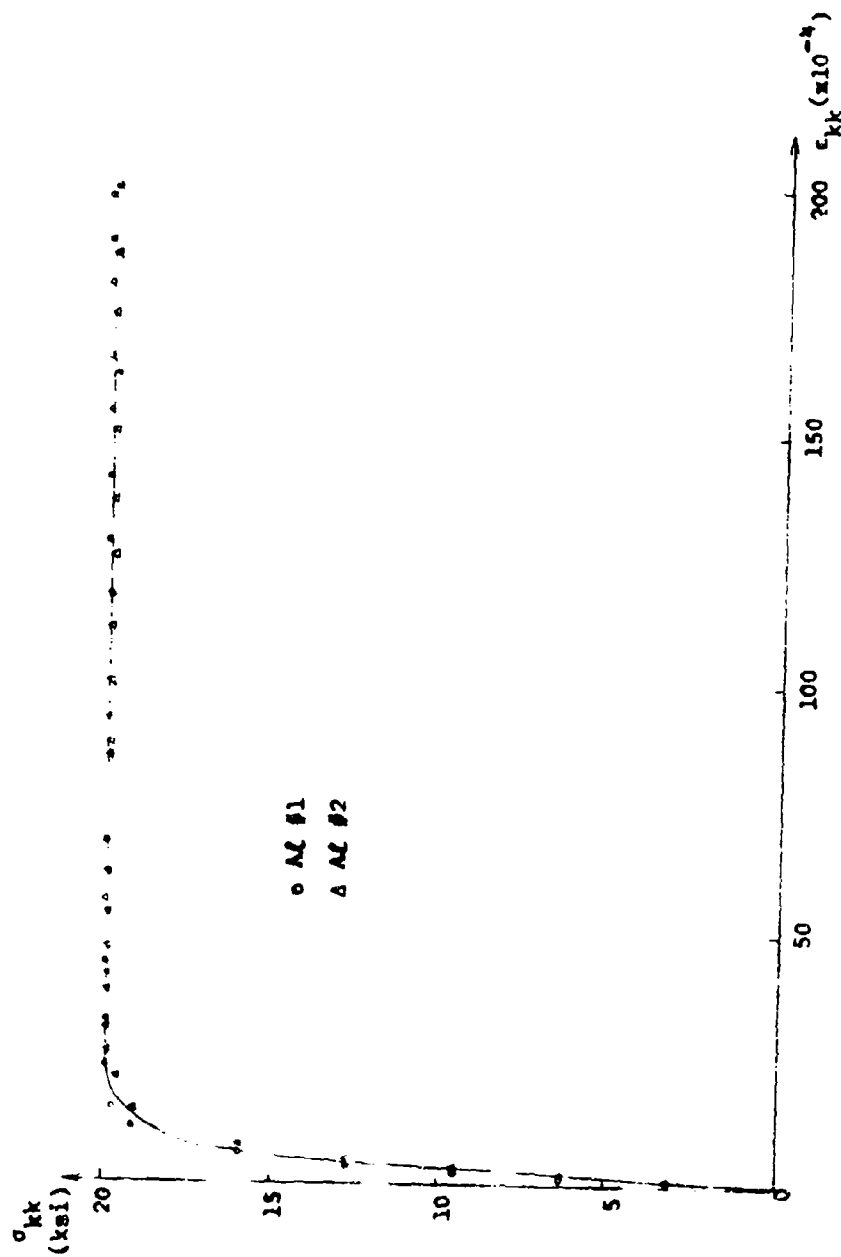


Figure 3 Hydrostatic stress ( $\times 3$ ) versus  
volumetric strain for aluminum of group I

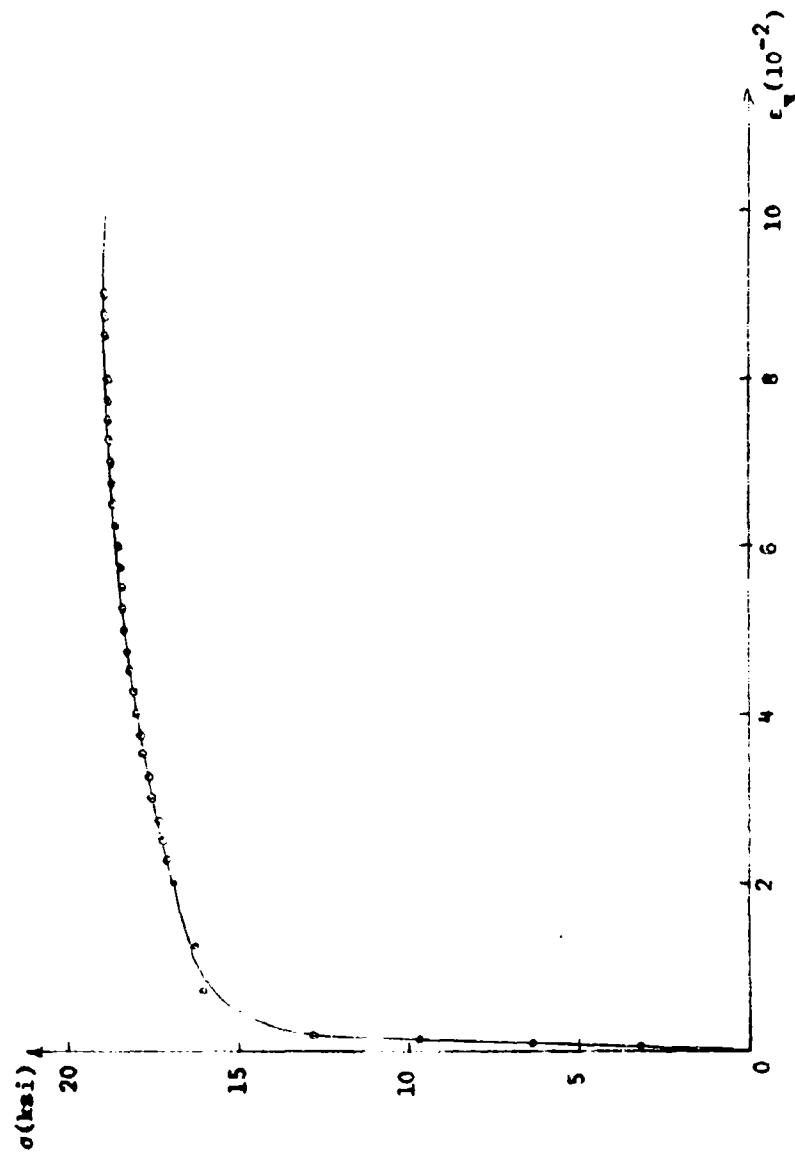


Figure 4 The stress-strain curve for aluminum of group II

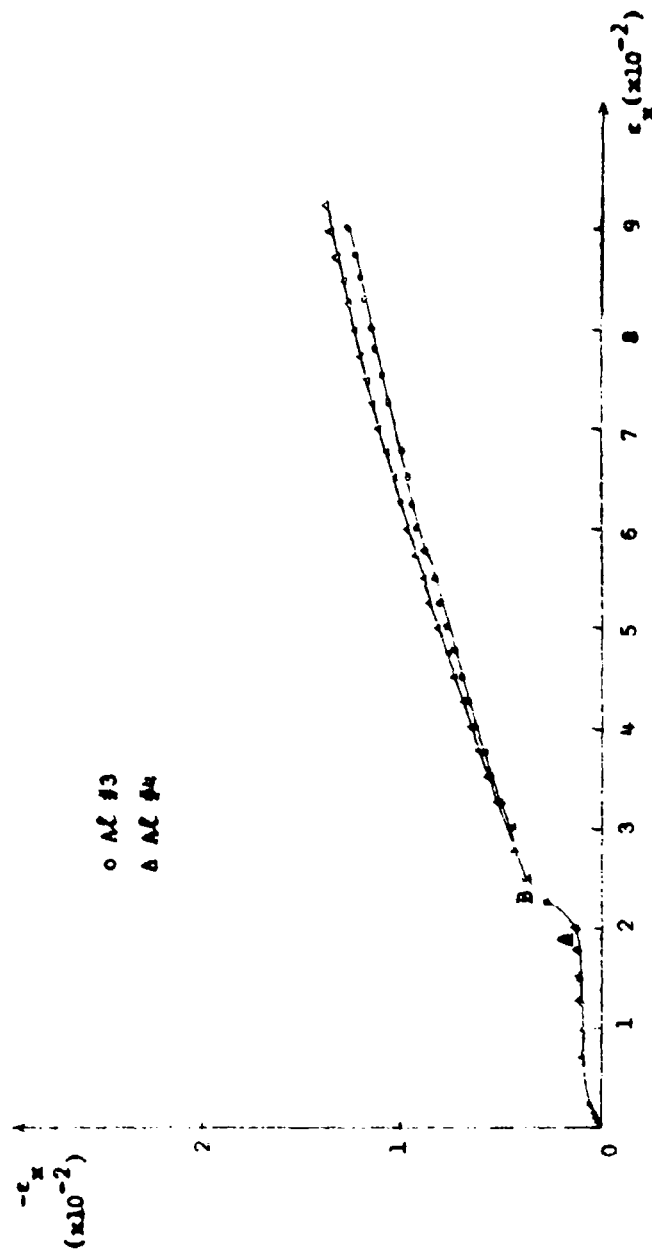


Figure 5 Relations between transverse and longitudinal strain for aluminum of group II

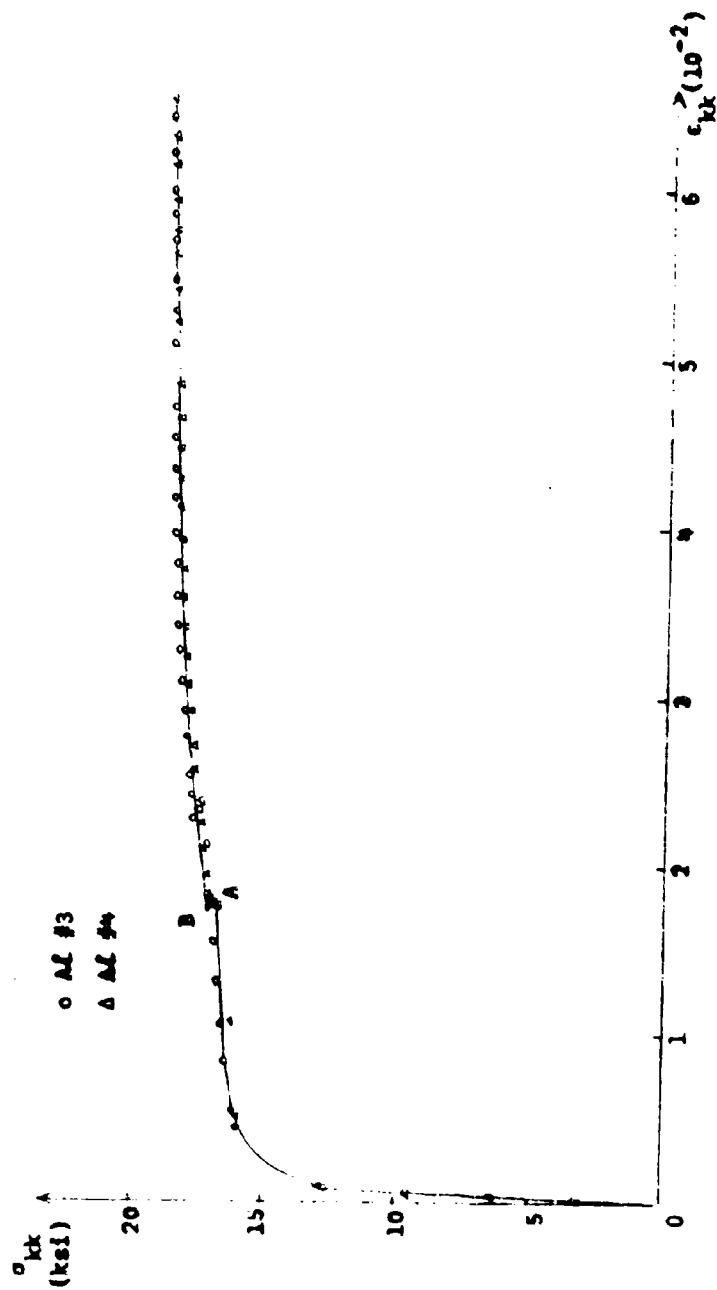


Figure 6 Hydrostatic stress ( $\sigma_h$ ) versus  
volumetric strain for aluminum of group II

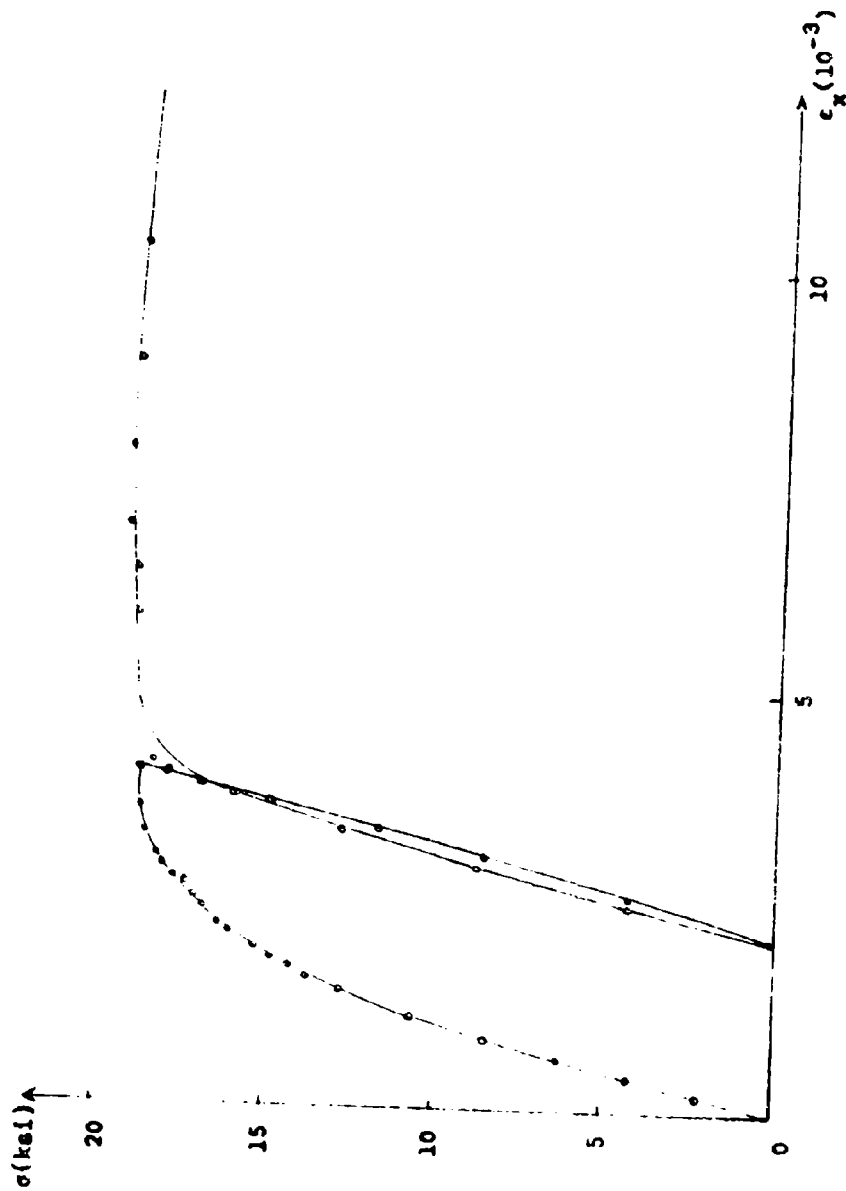


Figure 7 The stress-strain curve of aluminum specimen #5

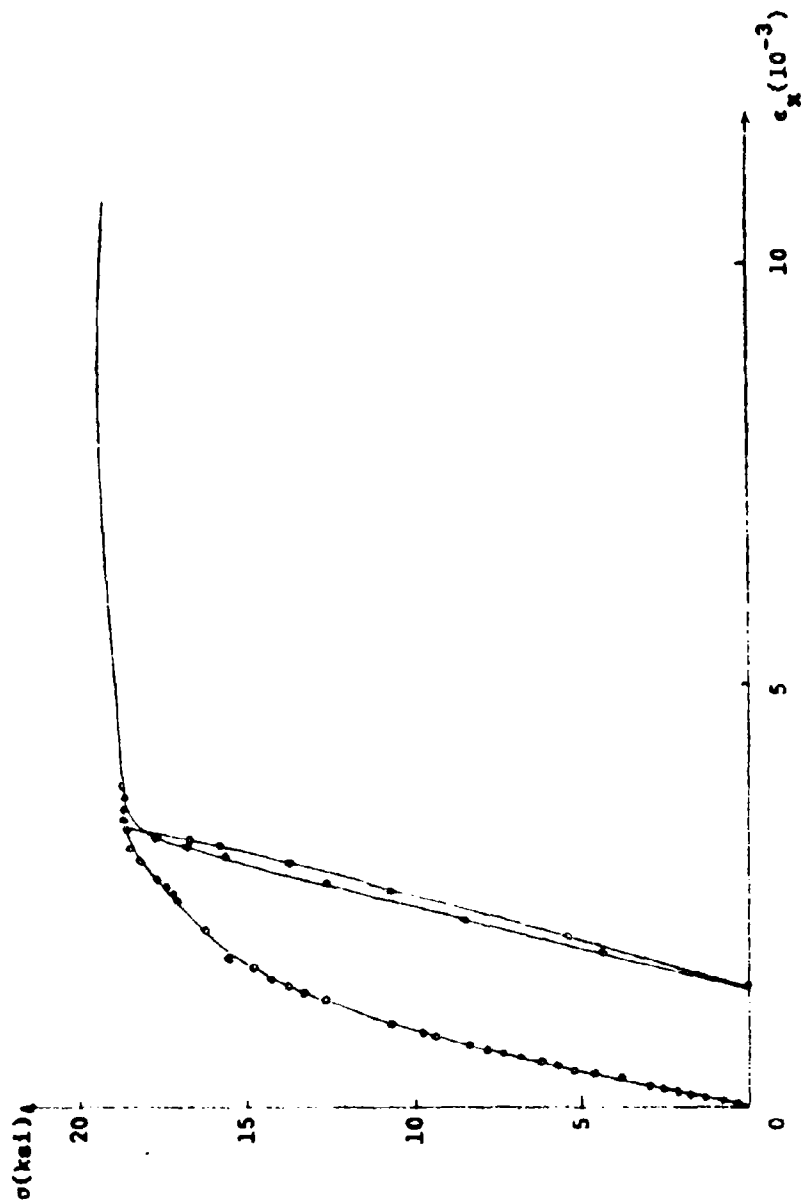


Figure 8 The stress-strain curve of aluminum specimen #6

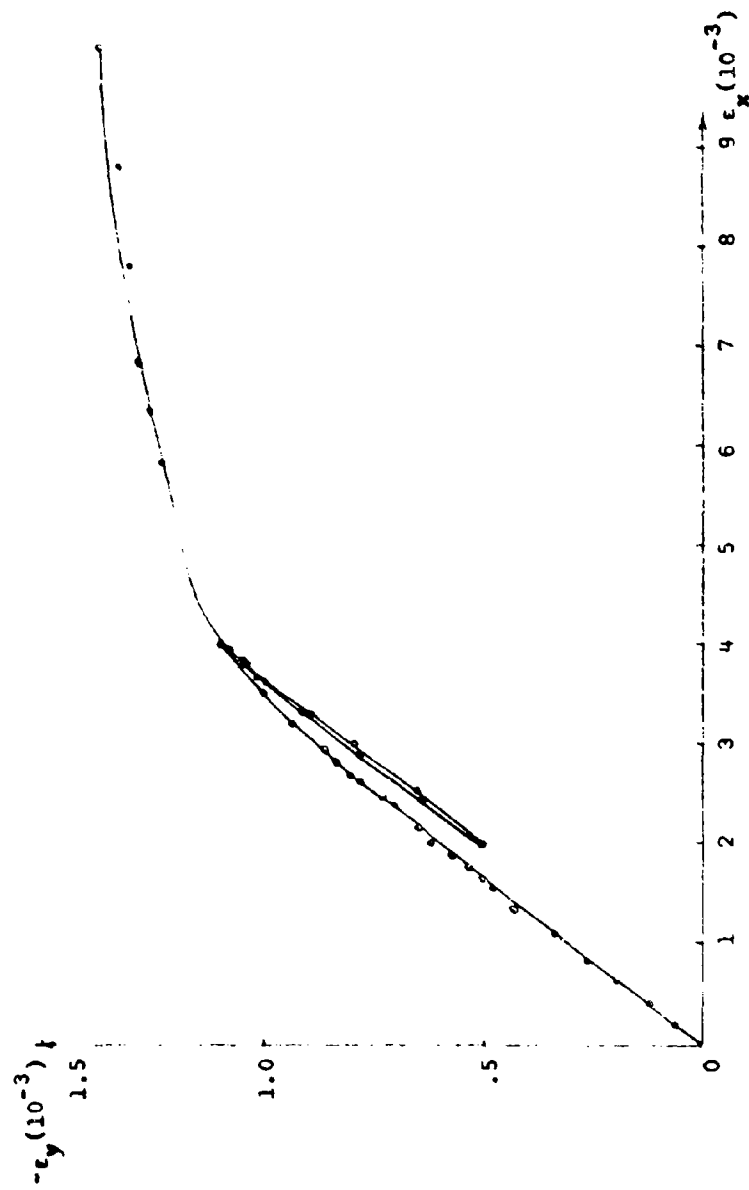


Figure 9 Relation between transverse and longitudinal strain for aluminum specimen #5

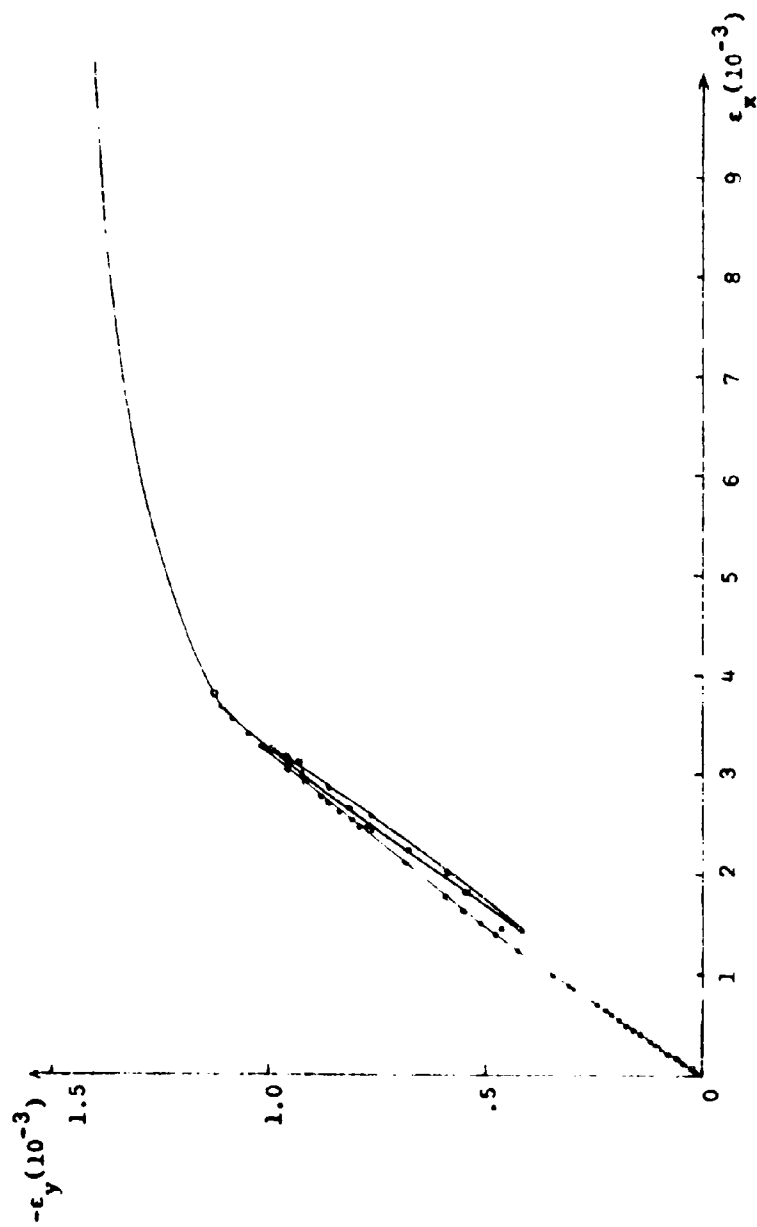


Figure 10 Relation between transverse and longitudinal strain for aluminum specimen #6



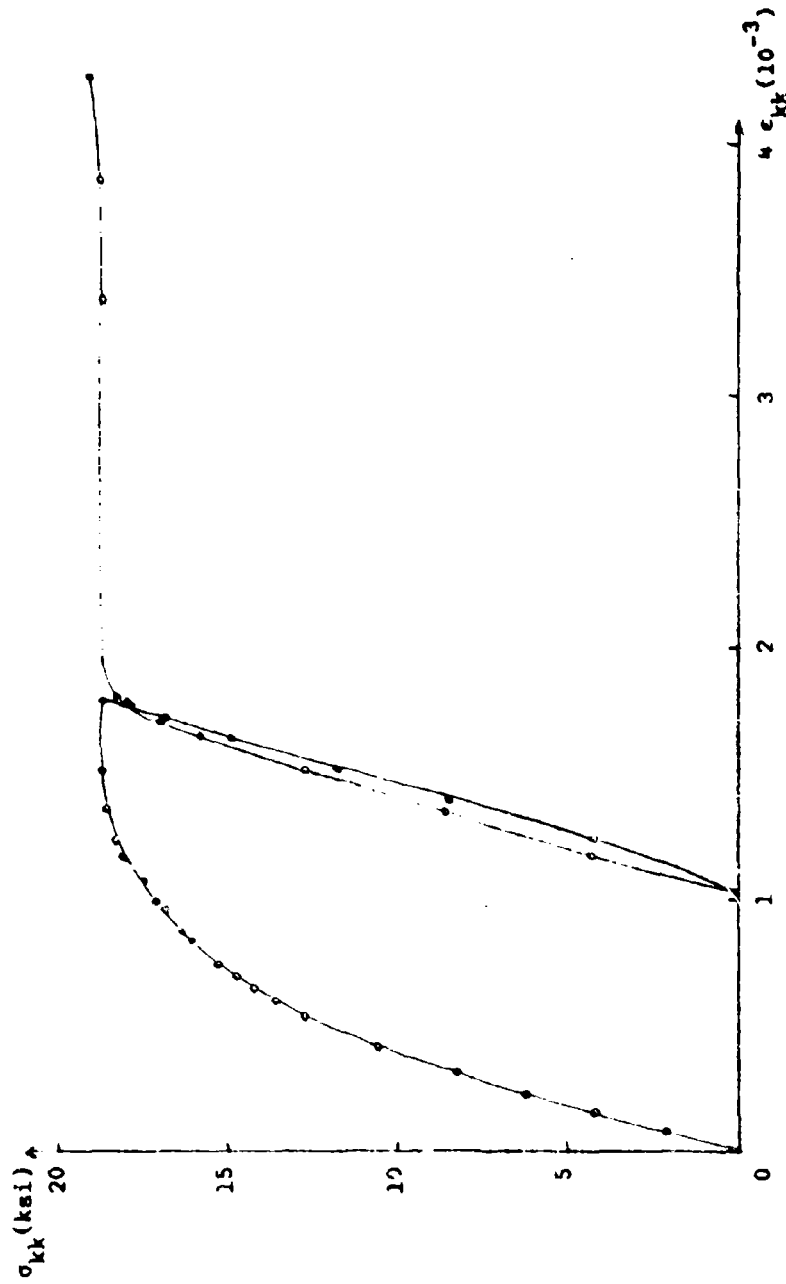


Figure 11 Hydrostatic stress ( $\times 3$ ) versus volumetric strain for aluminum specimen #5

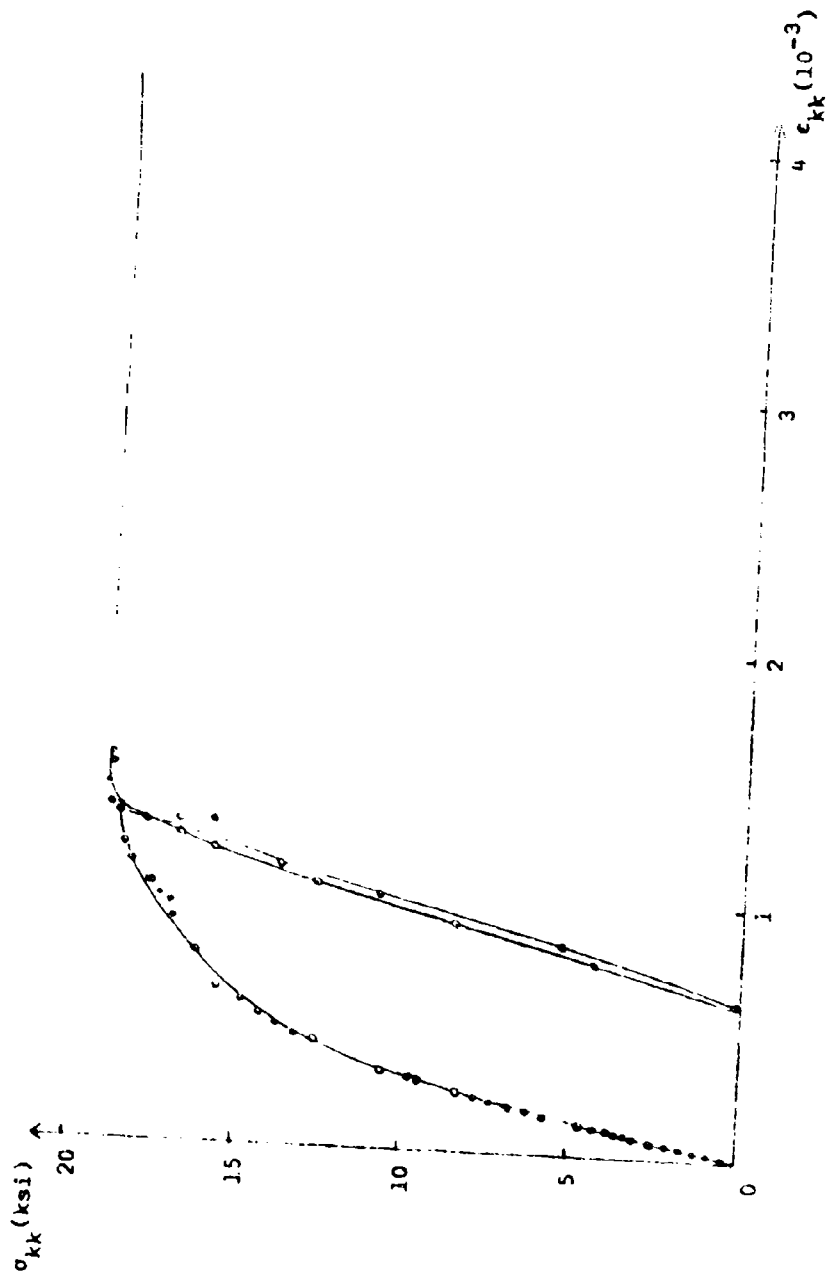


Figure 12 Hydrostatic stress ( $\times 3$ ) versus  
volumetric strain for aluminum specimen #6

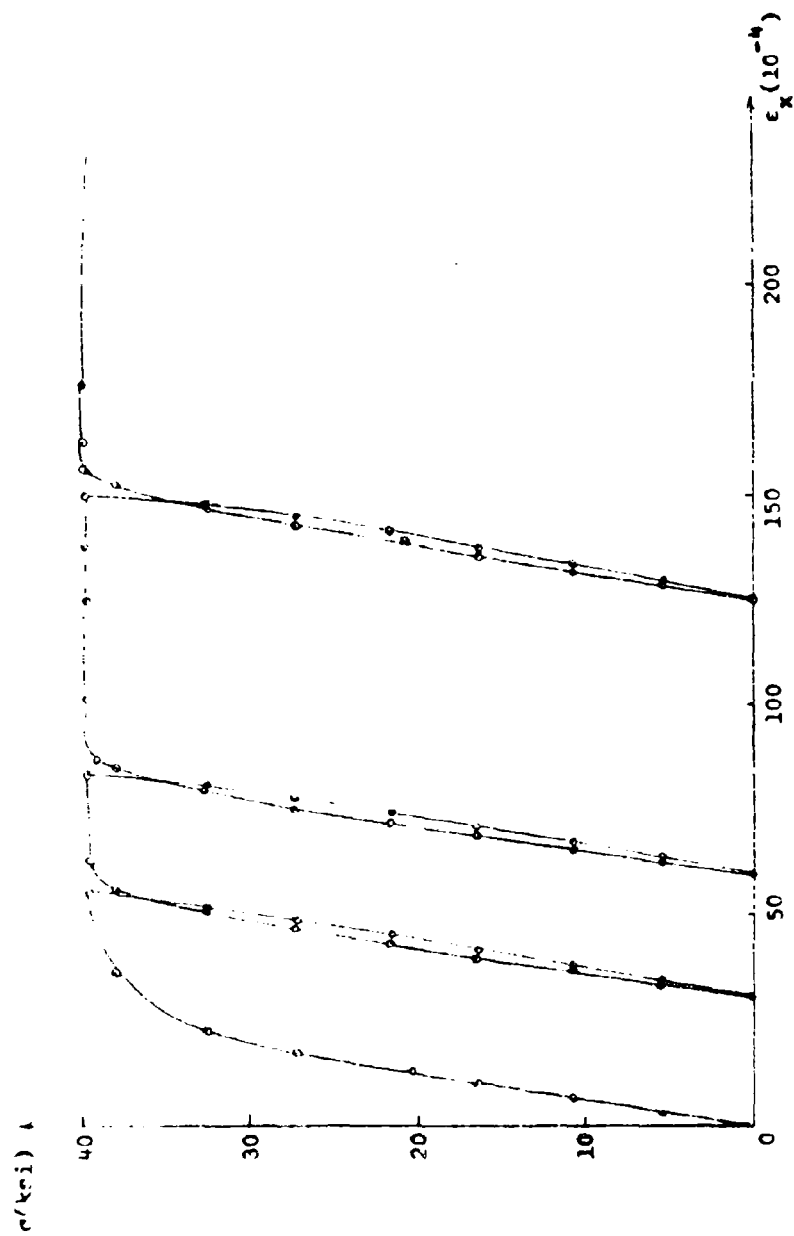


Figure 13 The loading-unloading  
curve for copper specimen #1

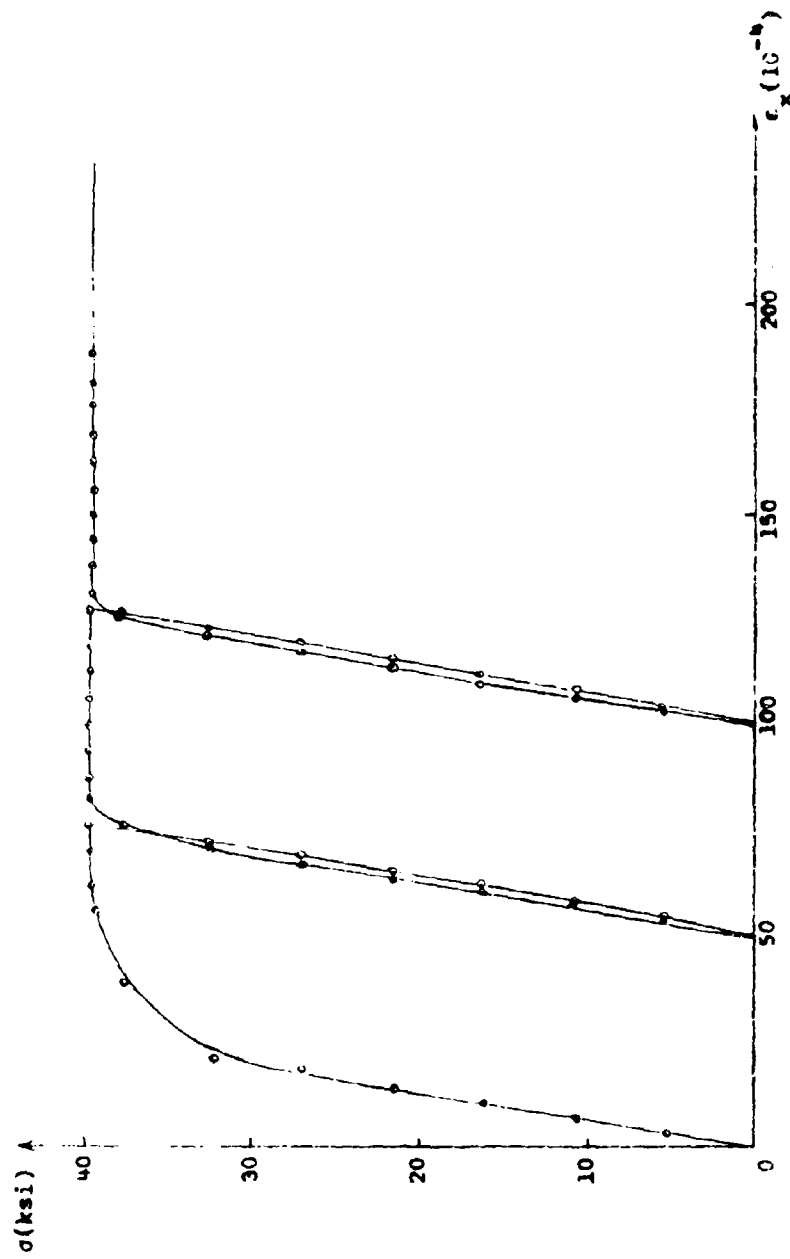


Figure 14 The loading-unloading curve for copper specimen #2

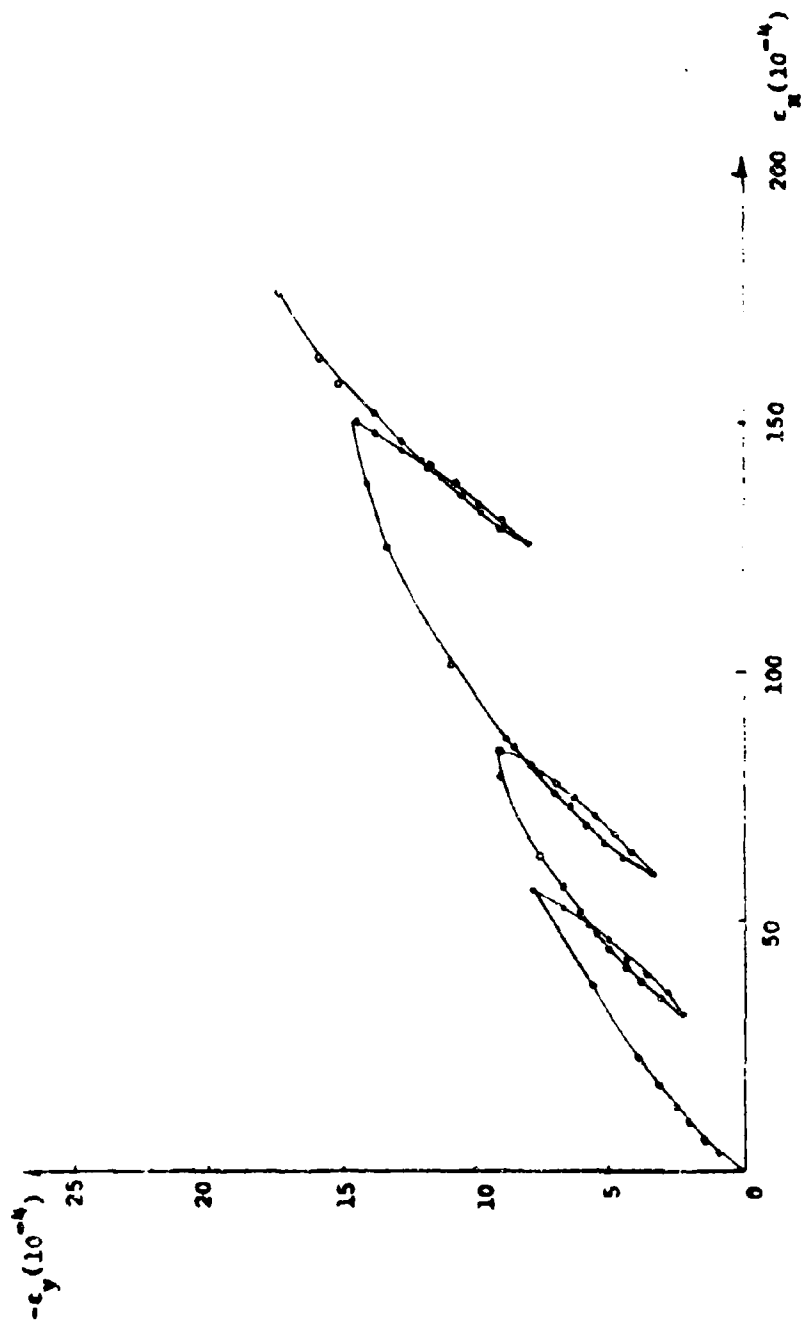


Figure 15 Relation between transverse and longitudinal strain for copper specimen #1

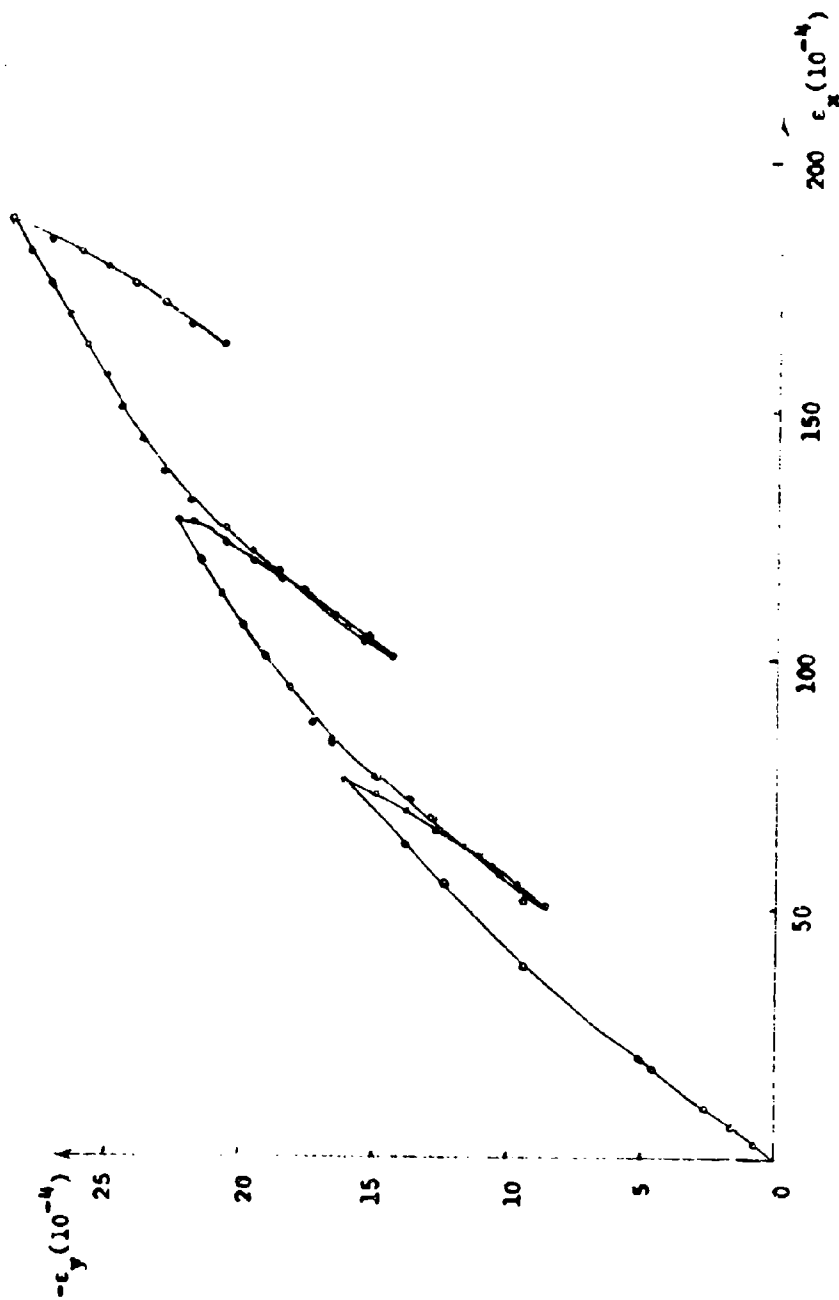


Figure 16 Relation between transverse and longitudinal strain for copper specimen #2

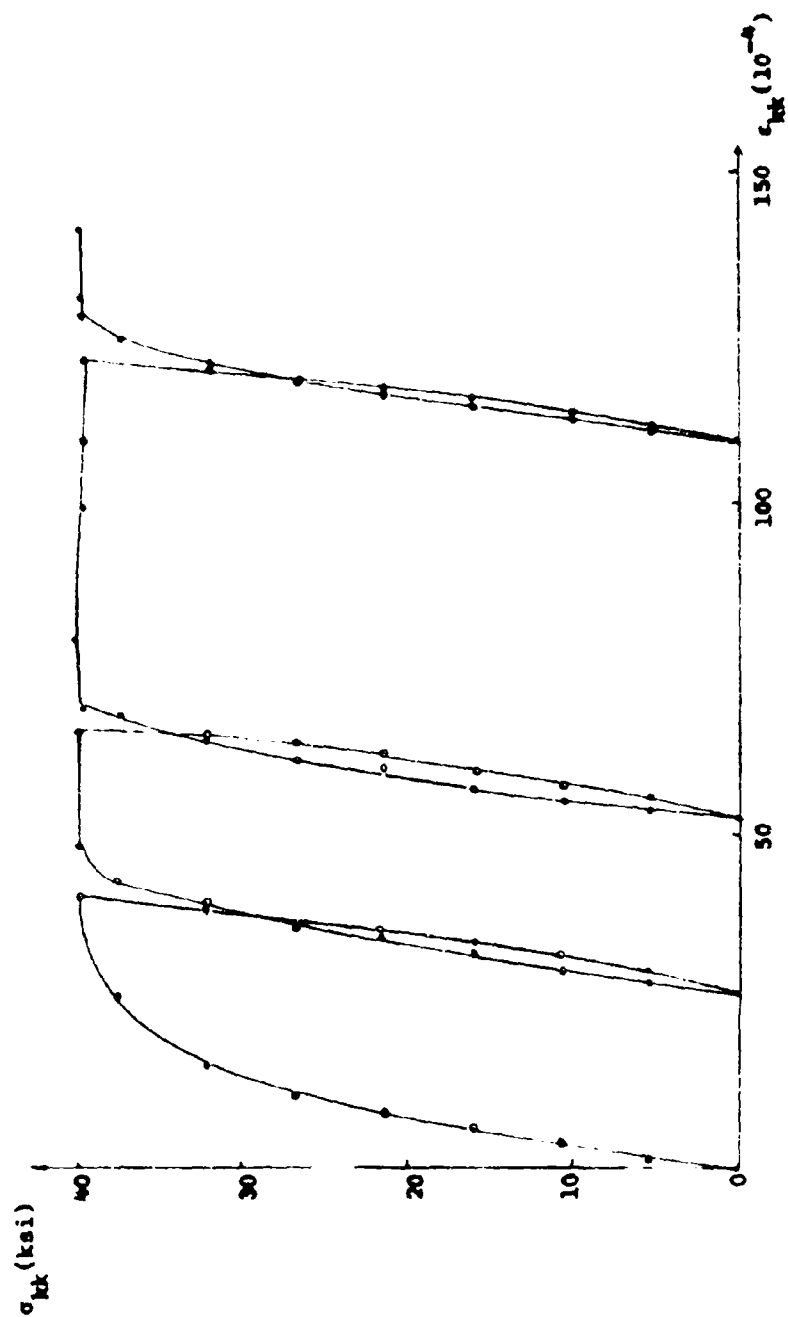


Figure 17 Hydrostatic stress ( $\times 3$ ) versus  
volumetric strain for copper specimen #1

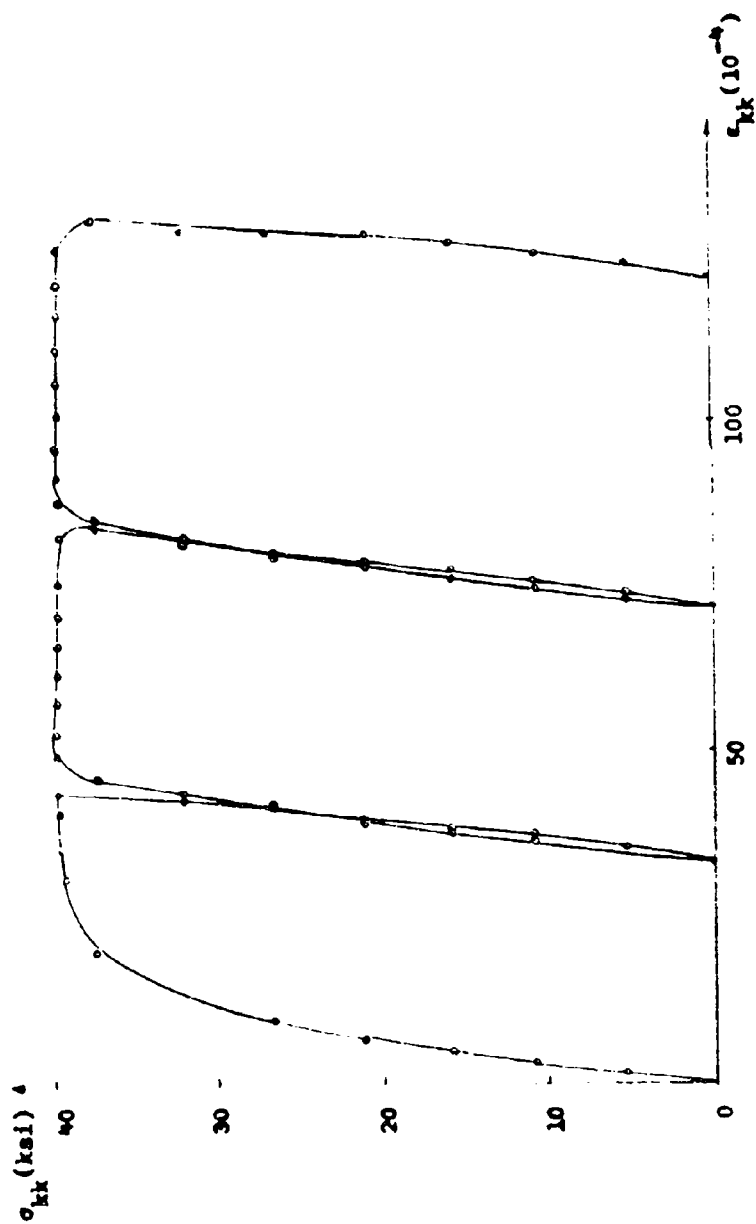


Figure 18 Hydrostatic stress ( $\times 3$ ) versus  
volumetric strain for copper specimen #2



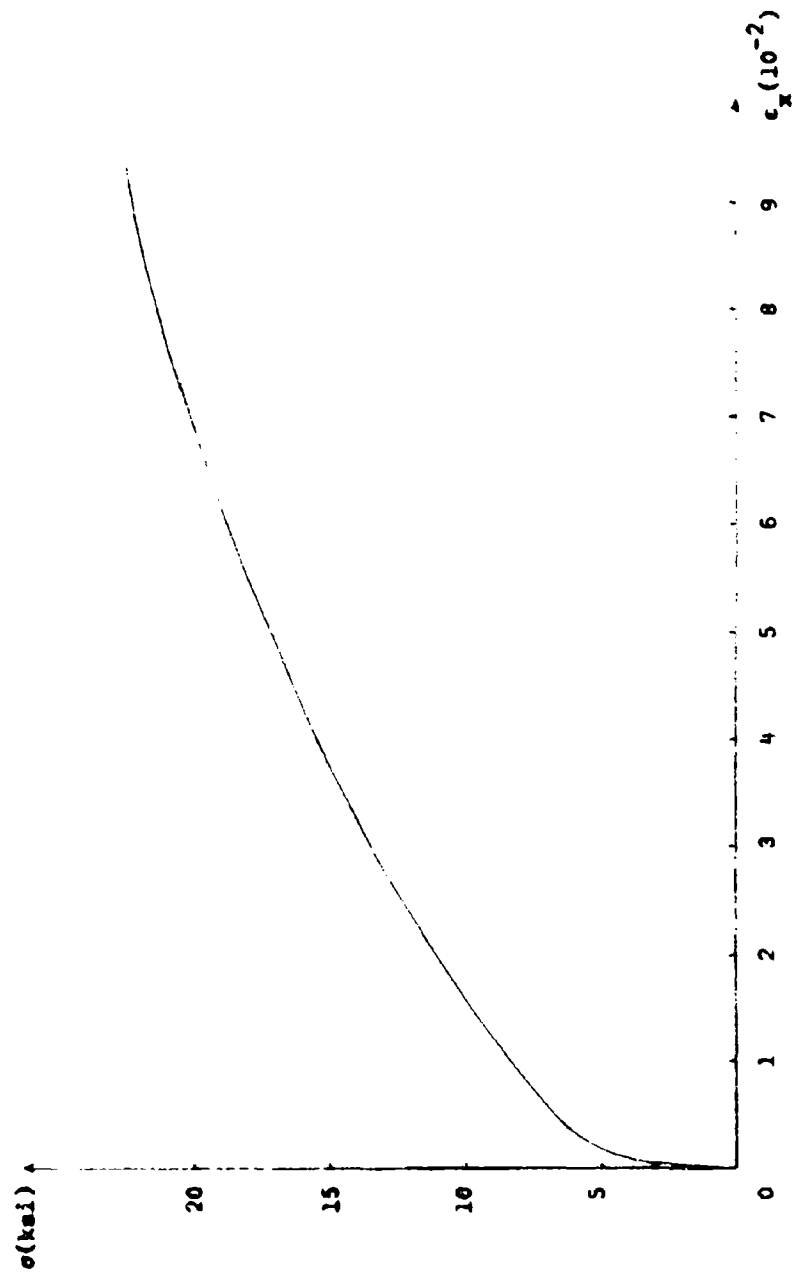


Figure 19 The stress-strain curve for copper of group II

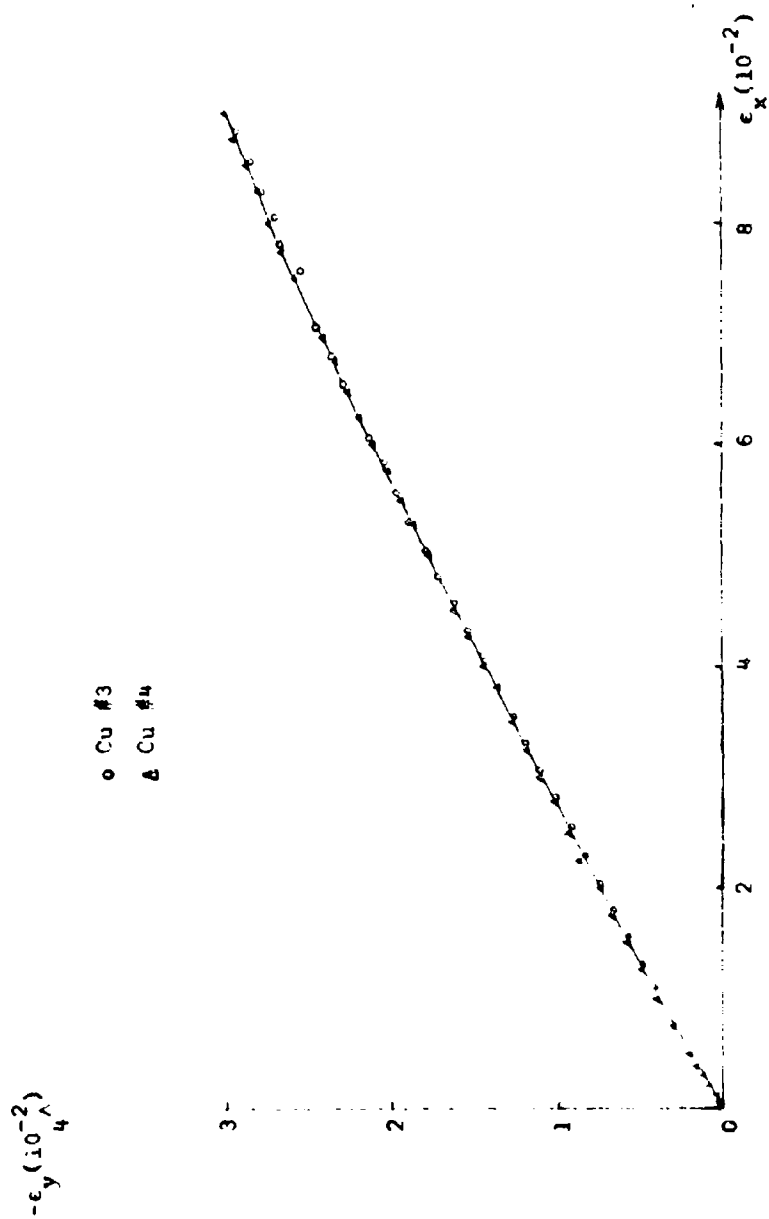


Figure 20 Relation between transverse and longitudinal strain for copper of group II

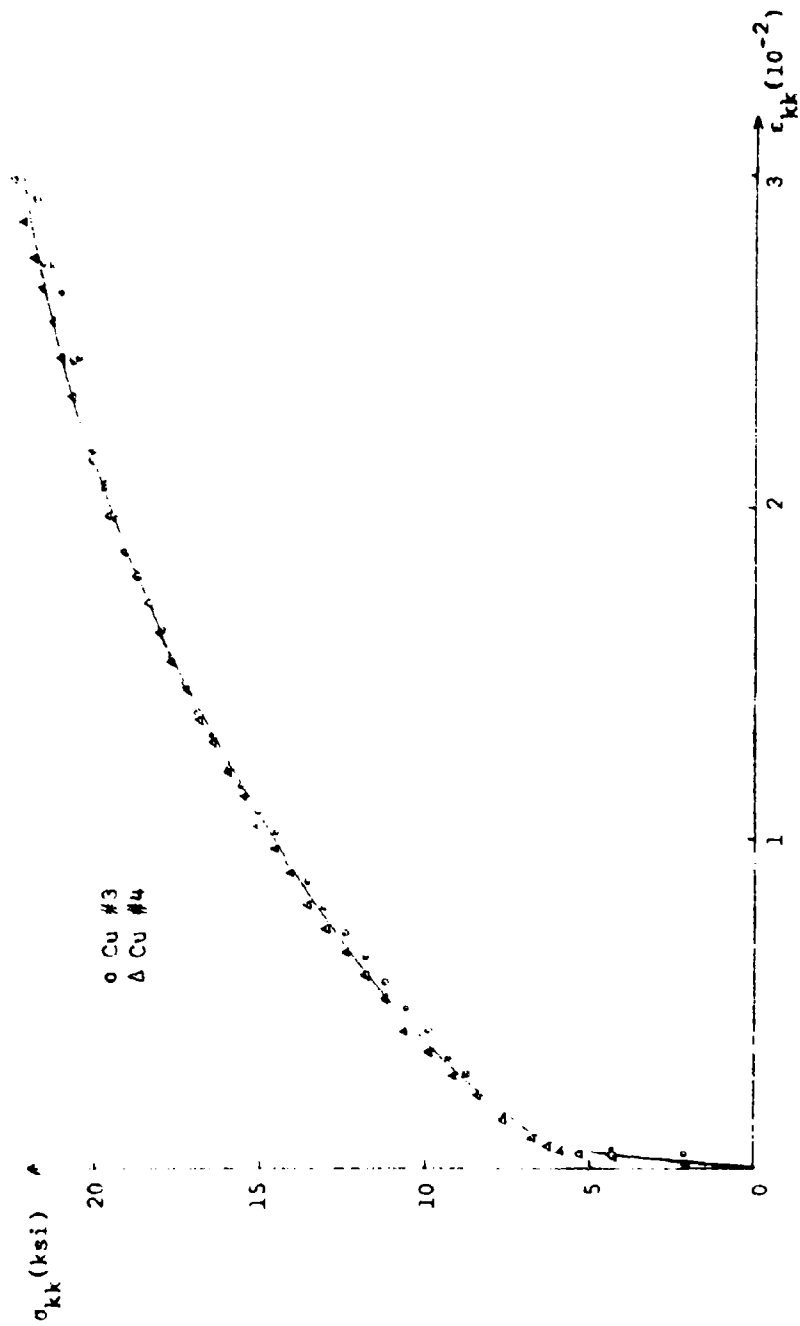


Figure 21 Hydrostatic stress ( $\times 3$ ) versus volumetric strain for copper of group II

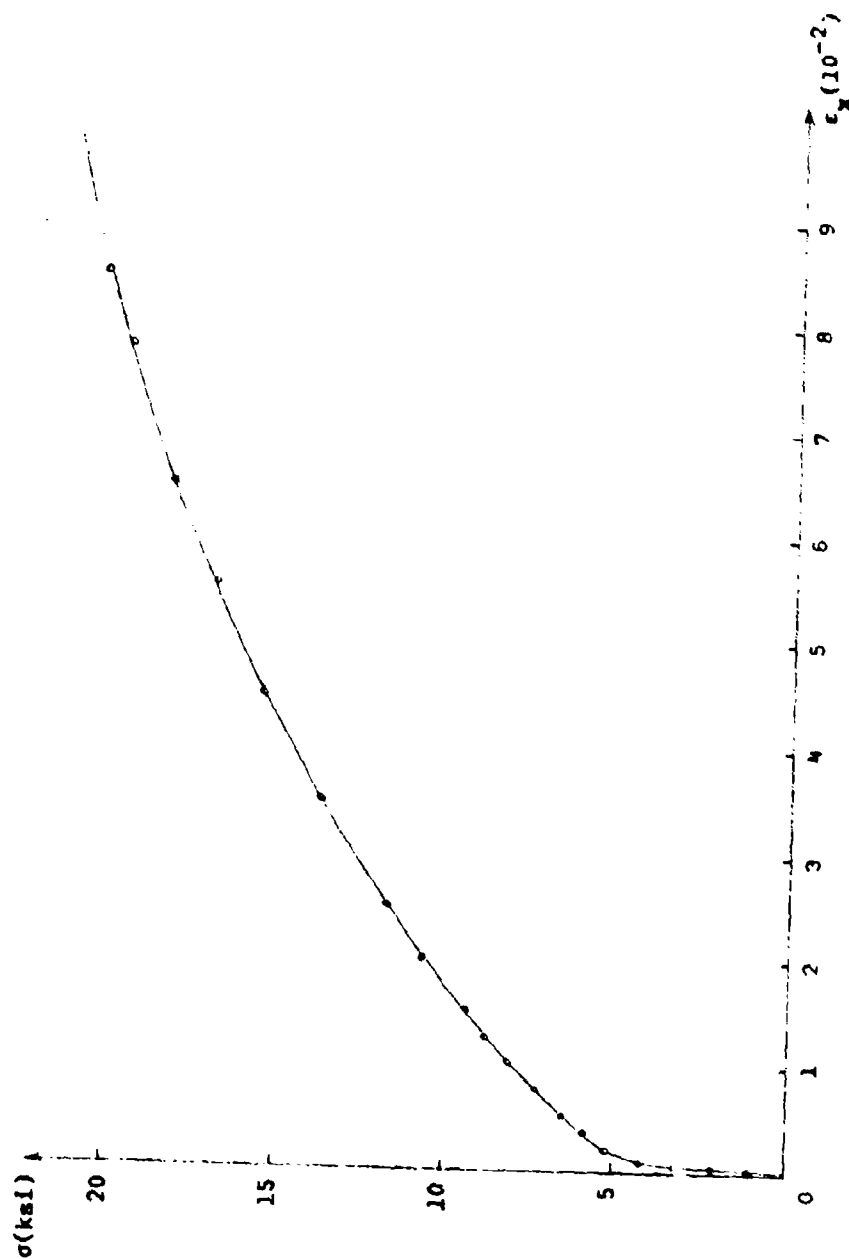


Figure 22 The stress-strain  
curve for copper of group III

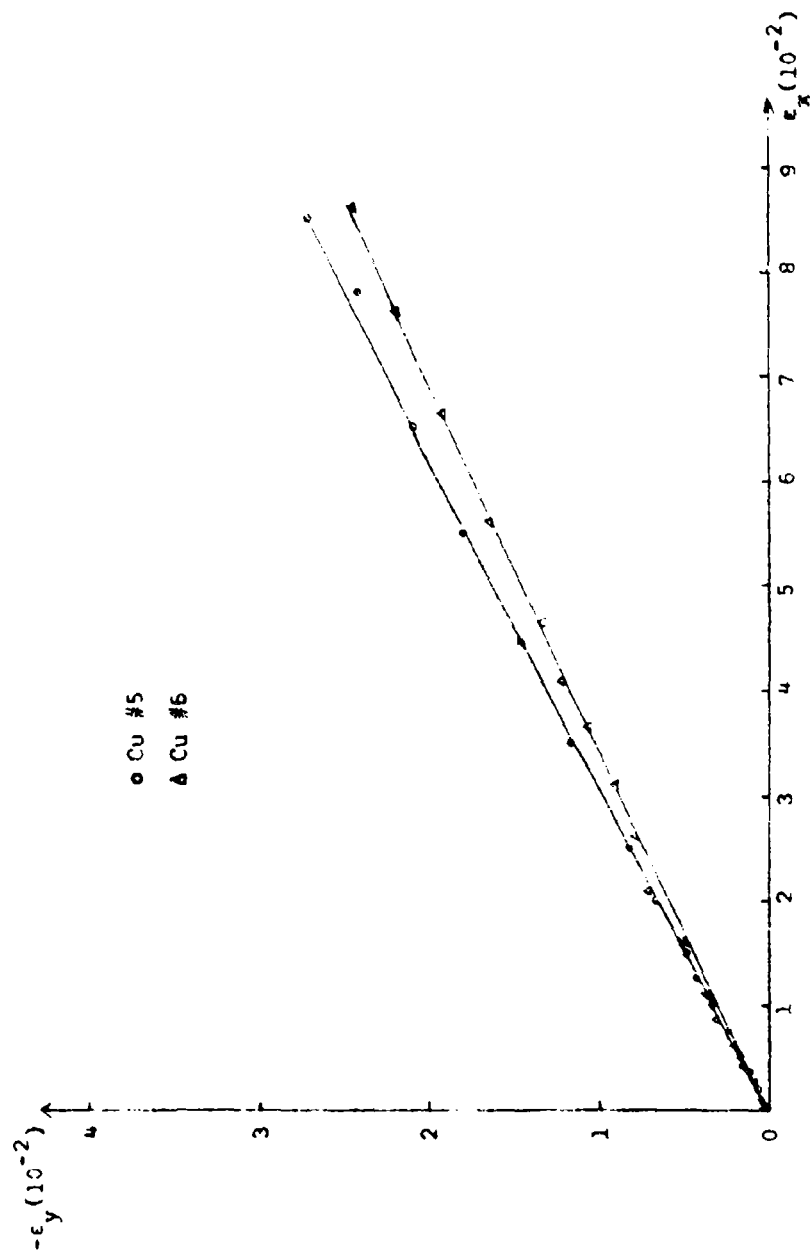


Figure 23 Relation between transverse and longitudinal strain for copper of group III

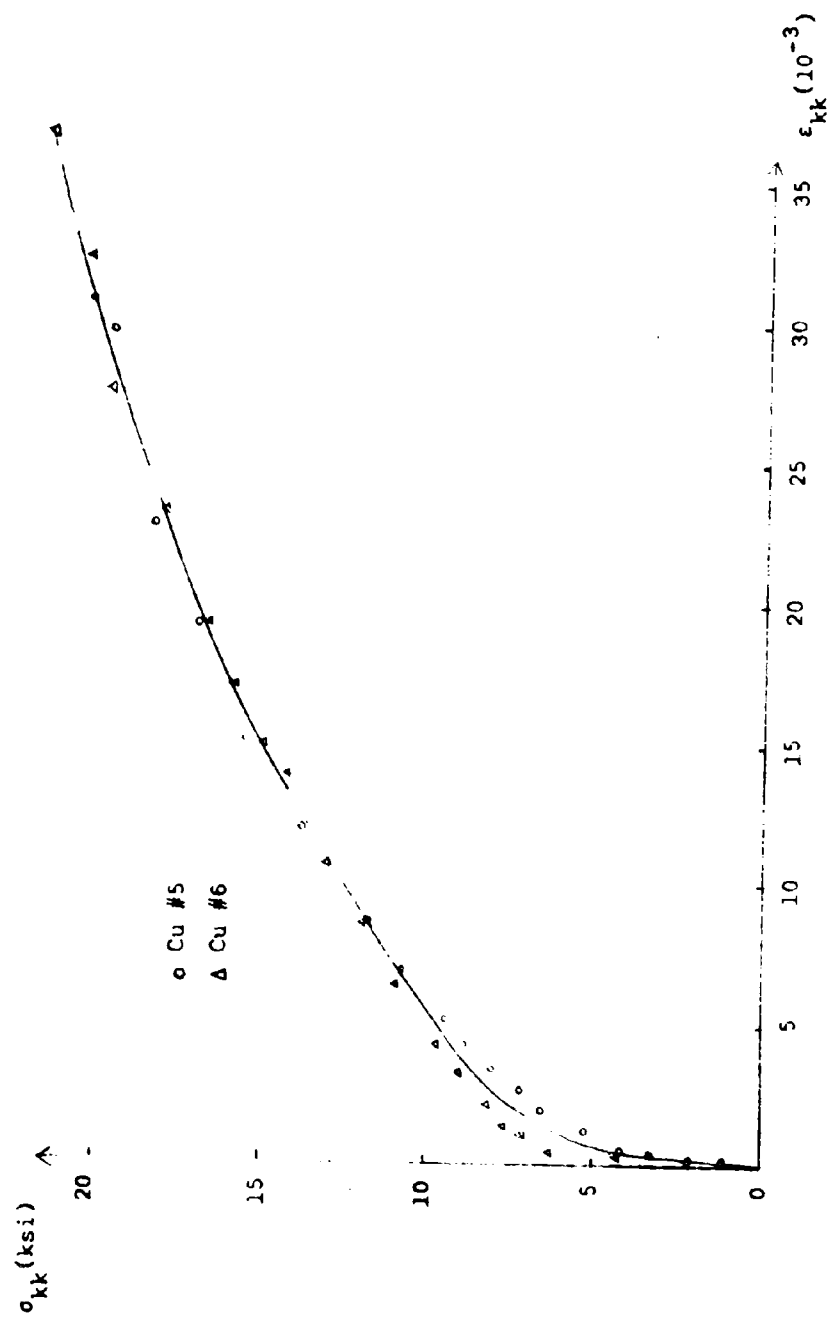


Figure 24 Hydrostatic stress ( $\times 3$ ) versus  
volumetric strain for copper of group II

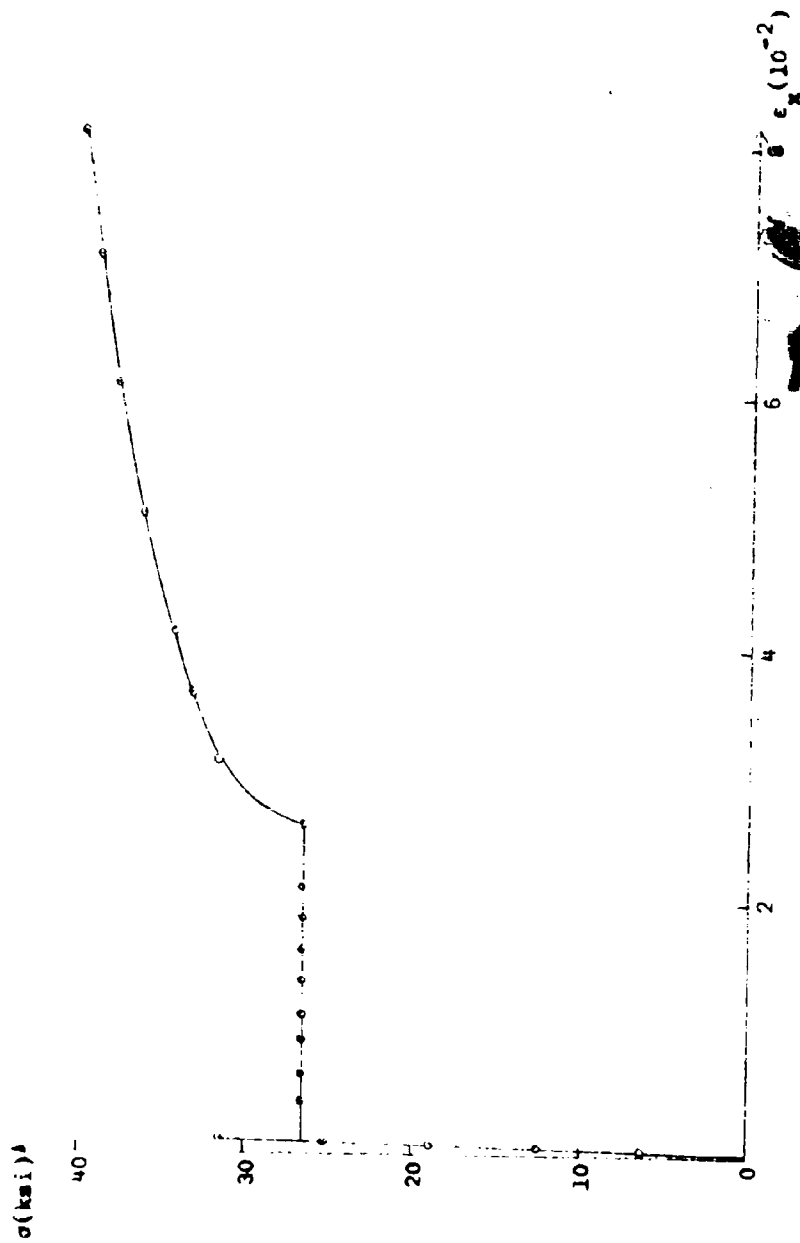


Figure 25 A typical stress-strain  
curve for low-carbon steel

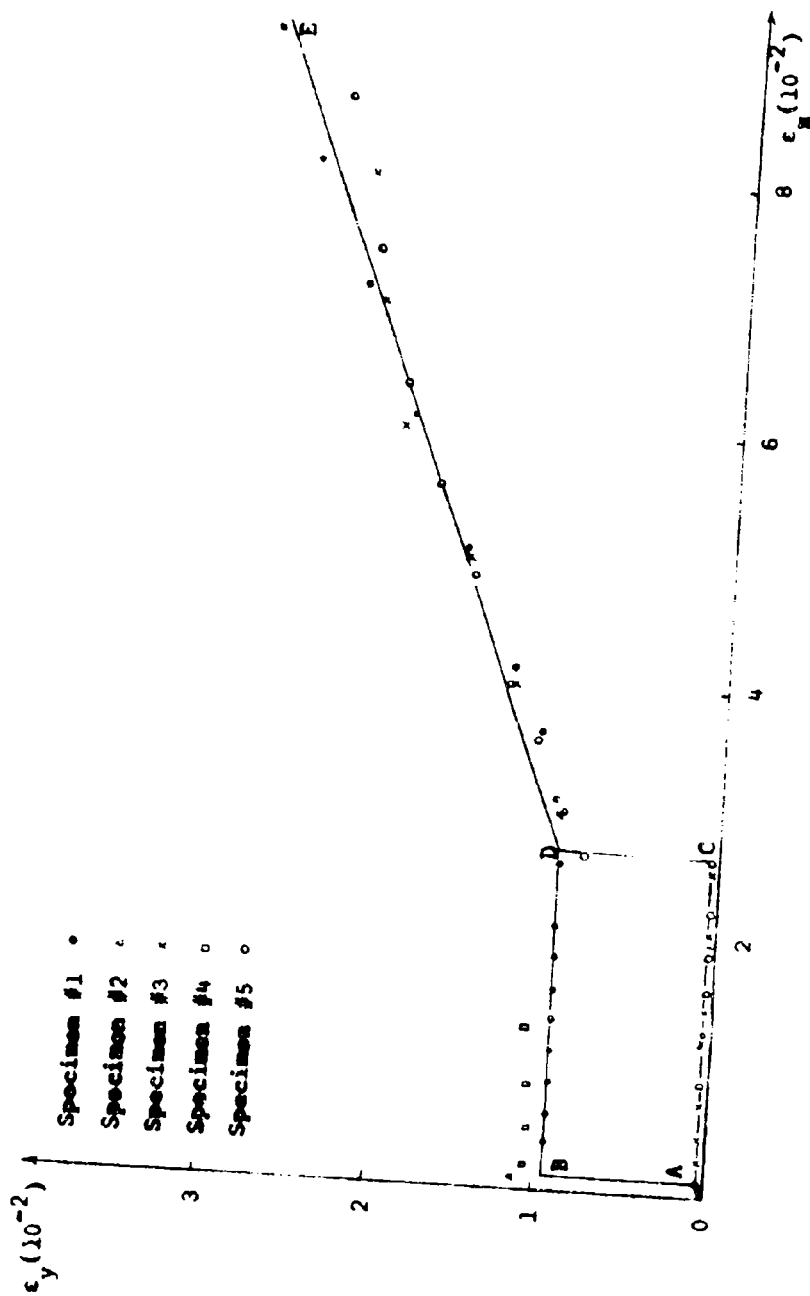


Figure 26 Relation between transverse and longitudinal strain for low-carbon steel



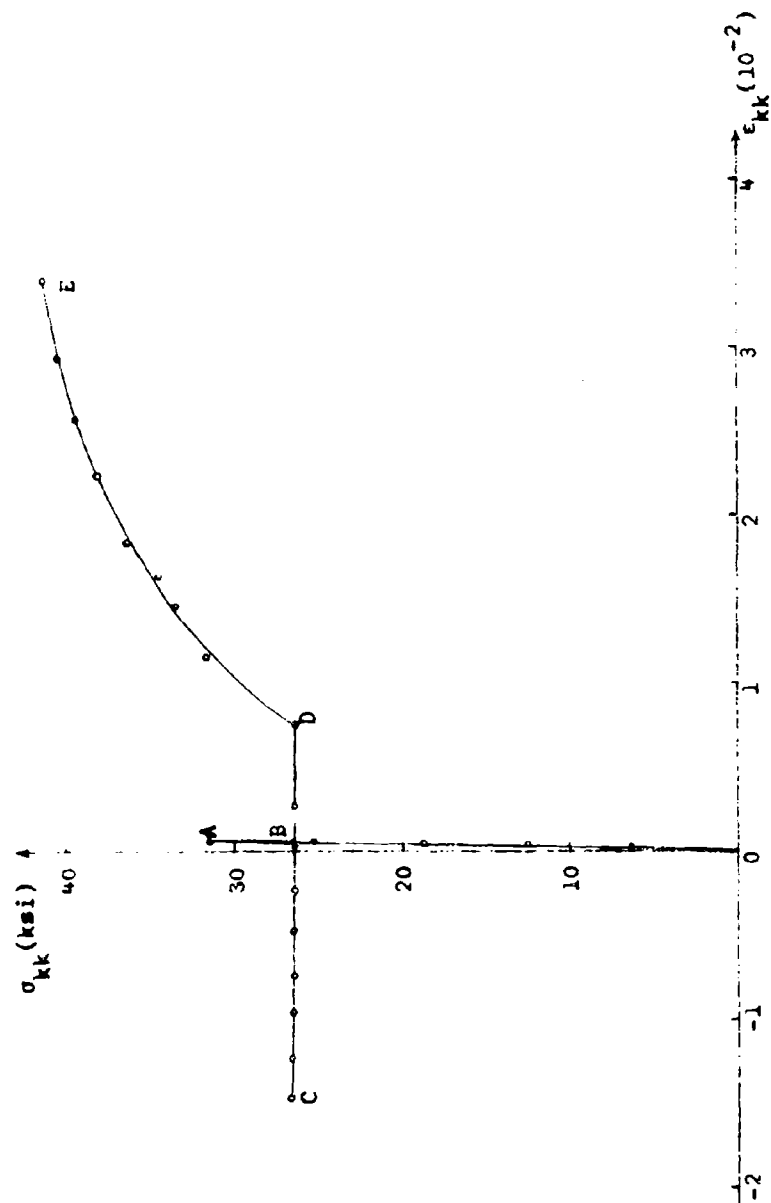


Figure 27 Hydrostatic stress ( $\times 3$ ) versus  
volumetric strain for steel specimen #1

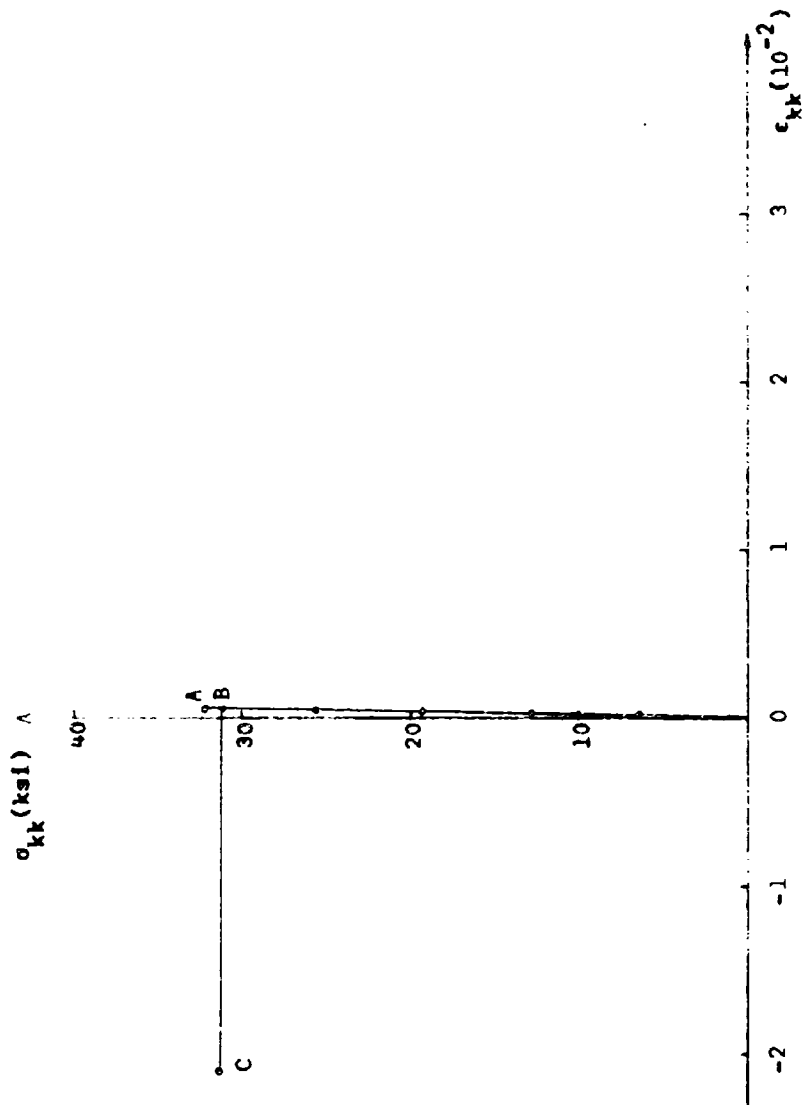


Figure 28 Hydrostatic stress ( $\times 3$ ) versus volumetric strain for steel specimen #2

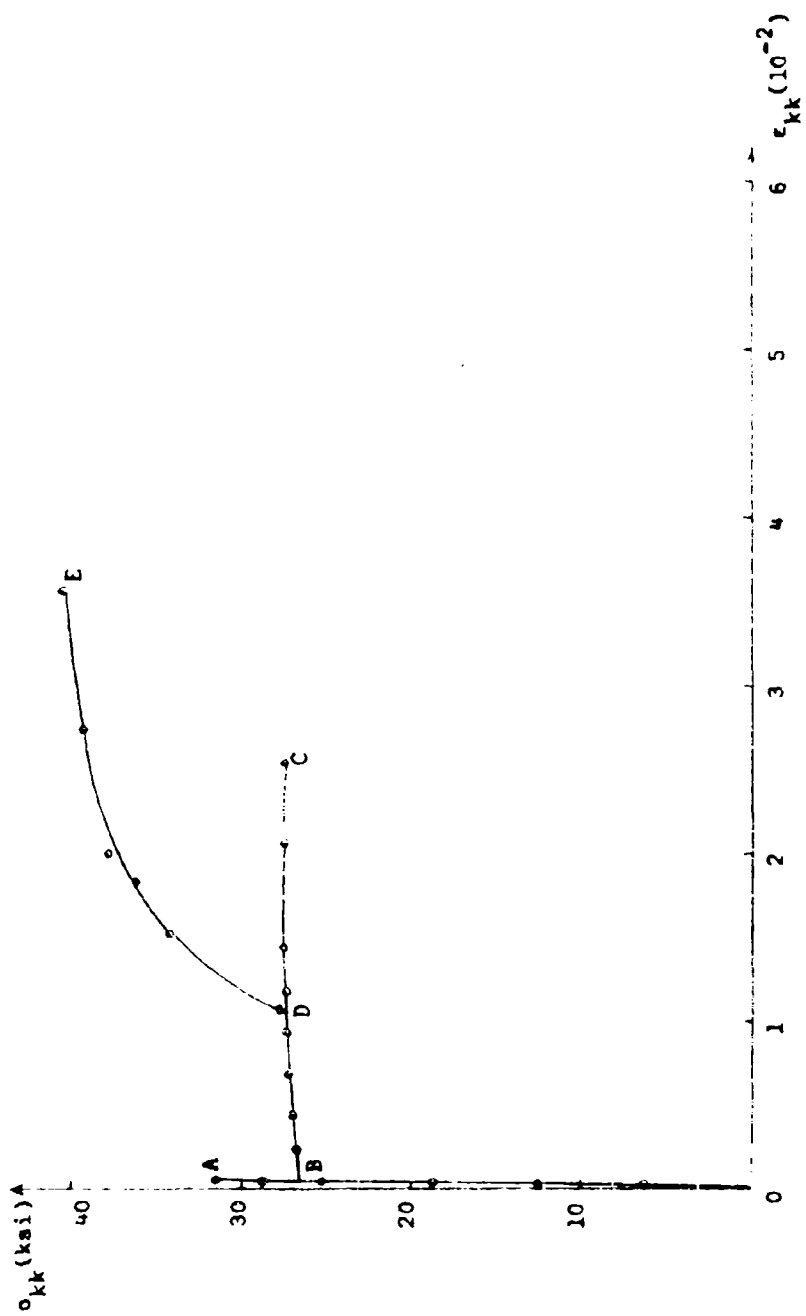


Figure 29 Hydrostatic stress ( $\times 3$ ) versus  
volumetric strain for steel specimen #3

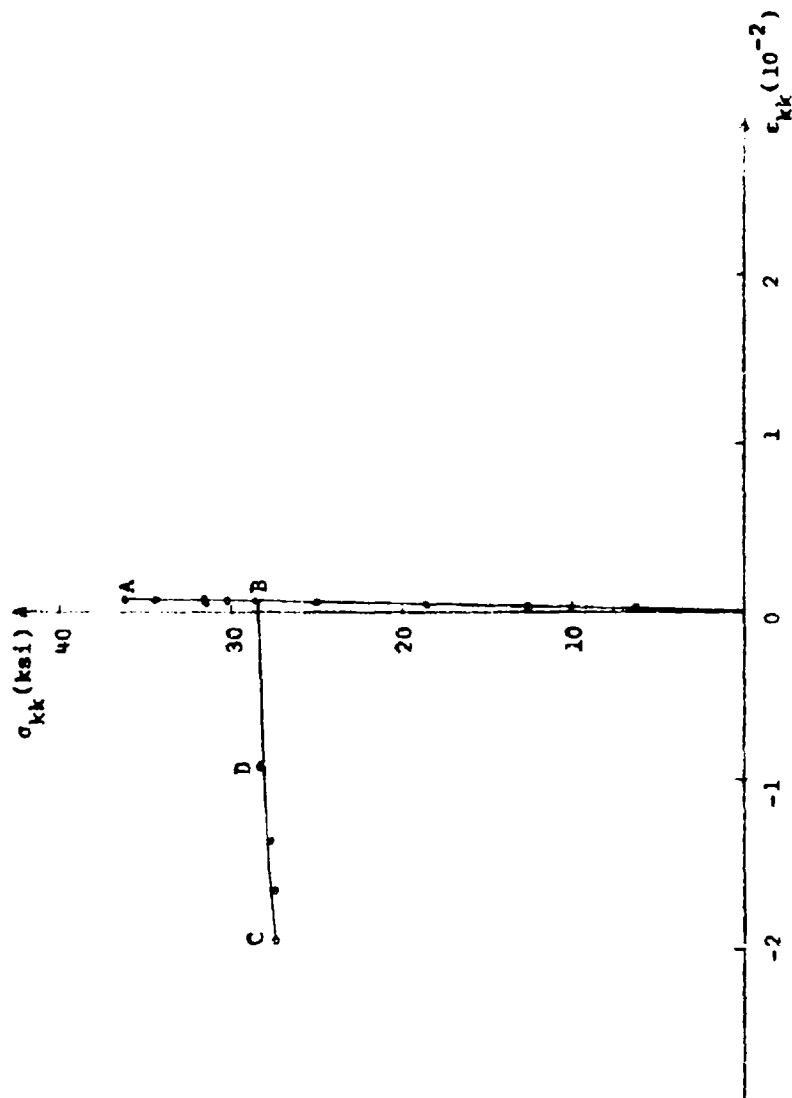


Figure 30 Hydrostatic stress ( $\times 3$ ) versus  
volumetric strain for steel specimen #4

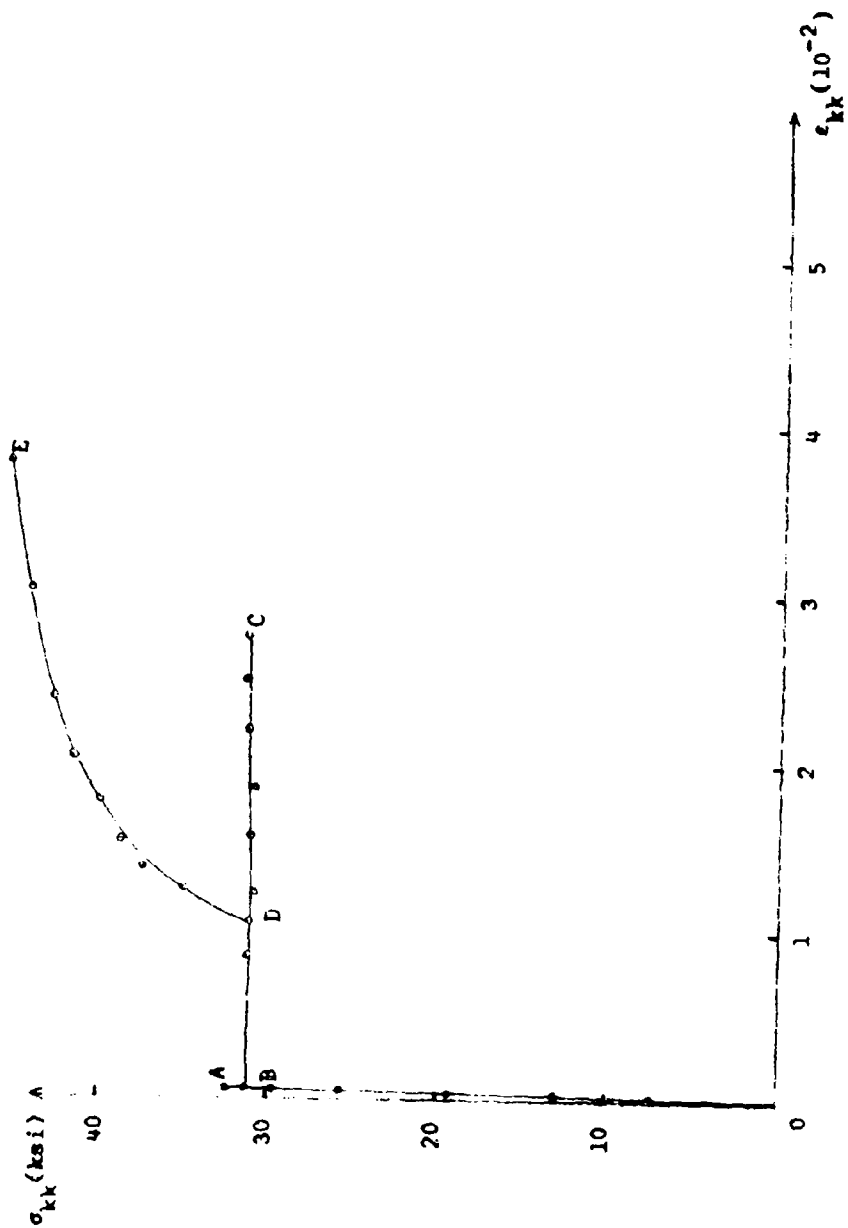


Figure 31 Hydrostatic stress ( $\sigma_{kk}$ ) versus volumetric strain for steel specimen #5